How do colloid separation and sediment storage methods affect water-mobilizable colloids and phosphorus? An insight into dam reservoir sediment

Diep N. Nguyen, Malgorzata Grybos, Marion Rabiet, Véronique Deluchat

How do colloid separation and sediment storage methods affect water-mobilizable colloids and phosphorus? An insight into dam reservoir sediment

Diep N. Nguyen, Malgorzata Grybos, Marion Rabiet, Véronique Deluchat

Limoges University, PEIRENE EA 7500, 123 Av. Albert Thomas, 87060 Limoges Cedex, France

Corresponding author: malgorzata.grybos@unilim.fr

Abstract

Despite the significant role played by colloids in determining the fate of contaminants in aquatic systems, obtaining knowledge about the mobilizable colloids from bottom sediments of dam reservoirs has not yet received sufficient consideration. A major obstacle to understanding the role of colloids in aquatic systems is the limited comparability of results with the literature due to the vast number of methods practiced for colloid extraction/separation and the various sample storage conditions used for colloid extraction purposes.

This work presents the effects of five colloid separation methods (namely direct filtration, successive filtrations, low-speed centrifugation and filtration, high-speed centrifugation and filtration, and successive centrifugations), combined with four sediment storage modes (wet, air-dried at 20°C, oven-dried at 40°C, freeze-dried), on the characteristics (mass, size distribution, composition) of water-mobilizable colloids from the bottom sediment of an eutrophic reservoir (Champsanglard, France). Special attention has been paid to phosphorus (P), an element that occupies a predominant place in the study of eutrophication process.

Results showed that Champsanglard sediment contained a relatively high stock of water-mobilizable colloids (over 5.4 g/$kg_{DW\text{-}Sed}$), along with the associated colloidal P constituted of approximately 4% total sedimentary P and 81% - 93% total water-mobilizable P (fraction < 1 µm). The mass and size distribution of released colloids, as well as the amount of colloidal and dissolved P, C_{org}, Fe, Ca, Mn, Al and Mg, differed by a factor of up to 26 depending on colloid separation protocols. The loss in colloidal mass upon membrane clogging during direct filtration was mitigated by means of a preliminary separation of particles through filtration and centrifugation, while successive centrifugations led to the potential overestimation of colloid quantity due to incomplete separation caused by presence of organic matter. Sediment storage impact at a greater extent on extracted colloidal mass. In comparison with fresh sediment, drying decreased up to 40 folds the amounts of colloidal and dissolved elements. Special attention should be paid to sediment storage and separation protocols. According to our results, the characterization of colloids shall be done on fresh sediment and with separation by successive filtrations or combination of centrifugation and filtration. The comparison between sediment of different reservoirs should be based on similar application of sample storage and colloid separation protocol, the definition of normalized protocol would be thus required. It is strongly advised to avoid using solely centrifugation for colloid recovery and sediment freeze-drying for long-term storage when working with sediments.

Keywords: Dam reservoir sediment, colloidal size distribution, colloidal composition, colloid quantity, phosphorus, separation, centrifugation, filtration, drying, freeze-drying.

Abbreviations:

AF4	Asymmetric flow field-flow fractionation
ANOVA	One-way analysis of variance
CFC	Continuous flow centrifugation
CFF	Cross-flow ultrafiltration
DIP	Dissolved inorganic phosphorus
FFF	Field-flow fractionation
ICP-MS	Inductively coupled plasma mass spectrometry
LQ	Limit of quantification
MP-AES	Microwave plasma-atomic emission spectrometer
P	Phosphorus
P_{WM}	Water-mobilizable P
S/L	Dry weight solid-liquid ratio
TOC	Total organic carbon
TP	Total phosphorus
UC	Ultra-centrifugation
UF	Ultra-filtration
UPW	Ultrapure water

Introduction

Natural colloids (operationally defined as particles within the size range from 1 nm to 1 µm) play a key role in the fate and behavior of nutrients and contaminants in aquatic and terrestrial ecosystems, given their ubiquity and reactivity (Buffle and Leppard, 1995a, 1995b; Lead and Wilkinson, 2006; Baken, Regelink, *et al.*, 2016; Gottselig *et al.*, 2017; Gu *et al.*, 2018; Yan *et al.*, 2017). Despite the significance of colloids in the balance of mobile nutrients in natural environment, the state of knowledge is rather poor regarding colloids in dam reservoirs and, more specifically, colloids being mobilized from the bottom sediments of these systems. It should be noted that reservoir sediments are generally enriched in biogenic elements since they are receptors of elements from both the surrounding catchments and internal recycling in the column water (Wildi *et al.*, 2004; Teodoru and Wehrli, 2005; Maeck *et al.*, 2013; Maavara *et al.*, 2015; North *et al.*, 2015; Orihel *et al.*, 2017; Hahn *et al.*, 2018; Pestana *et al.*, 2019; Palanques *et al.*, 2020). In addition, their specific hydrodynamics, which depends in part on the type of dam and how it is managed, can cause sediment resuspension and thus contribute to the release of particles, colloids and ions through vertical distribution to the overlying water (Gálvez and Niell, 1992; Buermann *et al.*, 1995; Effler and Matthews, 2004; Filstrup and Lind, 2010; Cavaliere and Homann, 2012; Zhang *et al.*, 2012; Cervi *et al.*, 2019).

The colloids in lake and reservoir water can be derived from several pathways, including inlet water, the detachment and/or resuspension from bottom sediments, breakdown of larger aggregates

(biological and inorganic debris) and/or *in situ* formation of mineral precipitates or organo-mineral associations. In such systems, the increasing retention time promotes the entrapment and settling of fine and colloidal material, which for example in large lakes and reservoirs accounts for 30% of the inflowing suspended materials (Vörösmarty *et al.*, 2003). The mobilization of colloids from bottom sediments to overlying water (i.e. internal colloid load) is associated with natural mechanical disturbances of sediment, or bioturbation (Pokrajac *et al.*, 2007; Valipour *et al.*, 2017; Phillips *et al.*, 2019; Schroeder *et al.*, 2019; Gautreau *et al.*, 2020). Mobilizable colloids from sediment may contain the colloids settled from the water column and/or colloids generated within the sediments. Many processes occurring within sediments may contribute to colloid generation, e.g. incomplete decomposition of organic debris (Wilkinson and Lead, 2007), mineral precipitation in sediment pore water (Lewandowski and Hupfer, 2005; Rothe *et al.*, 2014; Rothe *et al.*, 2016; Woszczyk, 2016; Steiner *et al.*, 2019; Vuillemin *et al.*, 2019) or aggregate disintegration by the dissolution of cementing agents (Newman, 2008; Henderson *et al.*, 2012). Colloids might also be continuously generated at the surface sediment-bottom water interface due to, for example: the mixing of reducing sediment porewater with overlying oxic water, and the oxidation of iron and manganese (Pakhomova *et al.*, 2007; Châtellier *et al.*, 2013; Corzo *et al.*, 2018).

Several protocols for extracting and separating colloids from various matrices (soil, sediment and water) have been proposed in the literature, including centrifugation and filtration (see Table 1). Sedimentation, membrane filtration and centrifugation are simple methods that have been used in many researches for studying aquatic colloidal particles over a long period and continuing through today (Table 1). Each approach has distinct advantages but also drawbacks. For example, conventional filtration with a 1-µm membrane may underestimate the mass of colloids and cause a serious error in the colloidal size class evaluation. A progressively clogged membrane during filtration involves a decrease in effective membrane pore size and thus retains colloids (Morrison and Benoit, 2001). On the other hand, centrifugation has been recommended for separating colloids due to its advantages in overcoming the entrapment or interaction of colloids with the filter membrane (Gimbert *et al.*, 2005). However, when operated properly in a way that avoids membrane overload and introduces multiple filters for large sample volumes (Morrison and Benoit, 2001), filtration can compromise high recovery.

Moreover, the differences in techniques used for colloid extraction, separation and characterization, plus the applied cutoff size could lead to differences in the colloidal size determination over the dissolved fraction. Conventional colloidal size separation has often been carried out at 1 µm for the upper colloidal fraction threshold, while the lower threshold for isolating colloids from the dissolved fraction has varied from one author to the next (Table 1). For example, Liu *et al.* (2014) considered a colloidal fraction of between 0.02 µm and 1 µm, whereas Tang *et al.* (2009) placed the size of this fraction at from 0.1 - 1.0 µm. In some instances, no distinction lies between dissolved and colloidal fractions (Gimbert *et al.*, 2006; Zirkler *et al.*, 2012; Yan *et al.*, 2017).

Regarding the widespread use of filtration, the problem of membrane clogging has been minimized by proceeding with the pre-removal of large particles, e.g. by: sedimentation (Tang *et al.*, 2009; Missong *et al.*, 2016), filtration at higher pore sizes (Gottselig *et al.*, 2017), centrifugation (Sinaj *et al.*, 1998; Turner *et al.*, 2004; Liang *et al.*, 2010; Zang *et al.*, 2013), and a combination of various techniques (Shand *et al.*, 2000). In addition, a wide range of colloid extraction methods are available; these comprise: the choice of solid-liquid ratio (w_{DW}/v) such as 1/8 (Missong *et al.*, 2018), 1/10 (Buettner *et al.*, 2014) and 1/20 (VandeVoort *et al.*, 2013), matrix type (soil, sediment, surface, groundwater) and its characteristics, and raw matrix treatment for storage before colloid extraction such as wet (Missong *et al.*, 2018), air-dried (Yan *et al.*, 2017), oven-dried (Regelink *et al.*, 2014) and

lyophilization (Xu *et al.*, 2019). The quantity of colloids in extracts varies from 0.03 to 1.7 g/L (Kaplan *et al.*, 1993; Yan *et al.*, 2017) and from 260 to 1,320 mg/kg (Sinaj *et al.*, 1998) in soil; from 122 mg/L (Tulve and Young, 1999) to 200-2,400 mg/L (Murali *et al.*, 2012) in sediment; and 0.7-8.6 mg/L (Hart *et al.*, 1993) in water. Nonetheless, it remains unclear whether the differences in quantity of extracted colloids across studies have been induced by differences in sample characteristics or by the colloid extraction/separation/characterization protocols and raw matrix conditioning.

The majority of available studies have focused on surface and groundwater, porous media and soils (Grolimund *et al.*, 1998; Kretzschmar *et al.*, 1999; Ran *et al.*, 2000; Bradford *et al.*, 2002; Wolthoorn *et al.*, 2004; Murali *et al.*, 2012; Baken *et al.*, 2016; Yan *et al.*, 2016; Gottselig *et al.*, 2017; Missong *et al.*, 2018). Much less attention has been paid to lake and river sediments (Seaman *et al.*, 1997; Tulve and Young, 1999; Murali *et al.*, 2012; Xu *et al.*, 2019) and among them, no identical protocol is observed.

The objective of this paper is twofold: 1) evaluate the role of various sediment storage modes (wet, air-dried at 20°C, oven-dried at 40°C, freeze-dried) and various colloid separation protocols (direct filtration, successive filtrations, low-speed centrifugation and filtration, high-speed centrifugation and filtration, successive centrifugations) on the characteristics (mass, size distribution and composition) of water-mobilizable colloids from reservoir sediment; and then 2) propose recommendations for future studies. All tests were performed on organic P-rich sediment sampled in a hydroelectrical dam reservoir located in a granitic catchment and periodically impacted by eutrophication (Champsanglard, France). Special attention was paid to the dissolved and colloidal P, by virtue of its key role in the algal bloom process (Zhang *et al.*, 2019).

Materials and methods

1. Sediment sampling and preconditioning

Sediment was collected in the middle channel of the Champsanglard dam reservoir (46°15'41.69"N, 1°53'30.49"E) on the Creuse River (France). This reservoir, with a surface area of 0.55 km², a total storage volume of 3.56 hm^3 and a water depth of up to 19.4 m, exhibits thermal and oxygen stratification along with a significant bloom of microalgae during the summer period (Rapin *et al.*, 2019b). Surface sediment (up to 10 cm) was collected from the reservoir bottom (approx. 9 m) during mid-May 2018 using an Ekman grab. The sediment was manually homogenized and preserved in polyethylene bottles previously rinsed with reservoir surface water. All bottles were kept in an icebox during transportation. In the laboratory, the wet sediment was immediately sieved through a 2-mm mesh and separated for four different conditionings: 1) one portion was kept at 4°C (denoted "wet"), 2) another portion was air-dried at ambient temperature (20° ± 1°C) for 2 weeks (denoted "air-dried at 20°C"), 3) another portion was dried in an oven at 40°C for 5 days (denoted "oven-dried at 40°C"), and 4) the last portion was freeze-dried using a lyophilizator (Cryotec, COSMOS-80) for 4 days (denoted "freeze-dried"). Table 2 presents the general physicochemical characteristics of this sediment.

The water loss on drying of sediment was determined as the percentage of mass loss after drying at 105°C until unchanged mass. The pH of sediment was measured on a suspension of wet sediment in ultrapure water with ratio of 1/1 (w/v) according to Method 9045D (US EPA 2015). The grain size (D50) of sediment was measured by laser diffractometer (MasterSizer 3000, Malvern) on wet dispersion under ultrasonic field in ultrapure water. Particle density was determined by drying a

certain volume of wet sediment at 105°C until unchanged mass. The particle density was then calculated as bulk density minus the pore spaces occupied by air and water according to following equation:

$$Bulk\ density\ (g/cm^3) = \frac{M\ dry\ sediment\ (g)}{V\ sediment\ (cm^3)}$$

$$Porosity\ (\%) = \frac{M\ moist\ sediment\ (g) - M\ dry\ sediment\ (g)}{1000 * V\ (L)} * 100\%$$

$$Particle\ density\ (g/cm^3) = \frac{Bulk\ density\ (g/cm^3)}{1 - Porosity\ (\%)}$$

The organic matter (OM) content was calculated by percentage of mass loss during calcination at 550°C for 2 h. The measurement of total P in sediment was performed according to the method of Ruban et al. (2001) in which calcinated sediment was digested with HCl 3.5 M for 16 h. Digested solution was centrifuged at 2000 g for 15 min, filtered through 0.45 µm cellulose acetate membrane (LLG Labware) and measured of dissolved phosphate by spectrophotometry (see part 3.2). The determination of total contents of Fe, Al, Ca, Mn and Mg was based on a microwave-assisted digestion procedure with concentrated peroxide (Merck, 30%), HNO_3 (Fisher, 65%) and HCl (Normapur, 37%) (Multiwave Go, Anton Paar) for 40 min at 180°C according to method 3015a (US EPA, 2007). The contents of Fe, Al, Ca, Mn and Mg in digested solution were determined by microwave plasma atomic emission spectroscopy (Agilent, MP-AES 4100) (See section 3.2).

2. Colloid extraction and separation

Throughout this study, the focus will be placed on the fraction of large colloids with a size ranging between 0.2 and 1 µm.

2.1. Extraction

Colloid extraction was carried out from sediment suspension prepared by adding 150 mL of ultrapure water (UPW) to a 15-g equivalent of wet sediment. The ratio of dried solid/liquid (S/L) equaled 1.7% (w_{DW}/v). Sediment suspensions were agitated for 24 h at 200 rpm using an orbital shaker (IKA-WERKE, KS 501 digital). Since drying involved significant sediment consolidation, before colloid extraction, the dried sediments were submerged in UPW for 2 days to soften, then gently hashed using a stainless spoon and shaken manually to disperse sediment particles. Dried sediments were not powdered so as to avoid a grinding process that would generate new colloidal particles.

2.2. Separation

The effect of the various colloid separation protocols was solely assessed on wet sediment.

Five such protocols were applied on the wet sediment in order to isolate the fraction smaller than 1 µm from sediment suspension. The separation protocols were selected according to reviews found in the literature (Gimbert *et al.*, 2005, 2006; Liang *et al.*, 2010; Murali *et al.*, 2012; Liu *et al.*, 2014; Regelink *et al.*, 2014; Séquaris *et al.*, 2013; Yan *et al.*, 2017), consisting of sedimentation, filtration, centrifugation or the combination of two techniques, as presented in Figure 1.

a) Direct filtration: Sediment suspension was decanted for 2 h by gravitation which allow to settle down large particles. According to the quality of decanting or centrifuging matters (mineral, organic or mix), the size cut-off would be different (Klitzke et al. 2012). Considering average

density of sediment, 2 h of decantation would settle the particles larger than 42 µm (d = 2.417 g/cm^3); for organic particles (d = 1.2 g/cm^3), the cut-off size would be 112 µm. then, the supernatant was filtered through a 1-µm filter. The cut-off size was calculated from equation (1):

$$d = \sqrt[2]{\frac{18\times\eta\times v}{g\times\Delta\rho}} \qquad (1)$$

where:
d: particle diameter (cm)
Δρ: difference in particle density and suspension medium (ρ_{water} = 1.0 g/cm^3)
η: dynamic viscosity of the suspension medium (η = 0.01 g/(cm.s))
v: settling velocity (cm/s)
g: gravitational acceleration (g = 9.81 cm/s^2)

b) Successive filtrations: Sediment suspension was filtered through 2.7 µm, and the filtrates were then passed through a 1-µm filter.

c) Low-speed centrifugation and filtration: Sediment suspension was centrifuged at 68 g for 15 min to separate particles larger than 2.0 µm (d = 2.417 g/cm^3). In case of organic particles (d = 1.2 g/cm^3), the cut-off size was 5.23 µm. The centrifugates were then carefully pipetted out and filtered through a 1-µm filter. The centrifugation speed and time were calculated using the equation (2), according to Gimbert *et al.* (2005):

$$t = \frac{18\eta\ln(R/S)}{\omega^2 d^2\Delta\rho} \qquad (2)$$

where:
d: particle diameter (cm)
Δρ: difference in particle density and suspension medium (ρ_p = 2.417 g/cm^3) (ρ_{water} = 1.0 g/cm^3)
η: dynamic viscosity of the suspension medium (η = 0.01 g/(cm.s))
t: settling time (s)
R: distance from the axis of rotation to the settling level in the tube (R = 10.8 cm)
S: distance from the axis of rotation to the suspension surface in the tube (S = 5.5 cm)
ω: angular velocity of the centrifuge (rad/s) as calculated by the following equation:

$$\omega = \frac{2\pi}{60}\times rpm$$

d) High-speed centrifugation and filtration: Sediment suspension was centrifuged at 272 g for 6 min to remove particles larger than 1 µm (d = 2.417 g/cm^3). In case of organic particles (d = 1.2 g/cm^3), the cut-off size was 2.62 µm. The centrifugates were then carefully pipetted out and filtered through a 1-µm filter.

e) Successive centrifugations: Sediment suspension was first subjected to centrifugation at 272 g for 6 min to remove the fraction greater than 1 µm (d = 2.417 g/cm^3) (Gimbert *et al.*, 2005). The supernatant was then gently pipetted out and submitted to the second centrifugation at 680 g for 6 min to settle the particles greater than 0.2 µm (d = 2.417 g/cm^3). In case of organic particles (d = 1.2 g/cm^3), the cut-off size would be 2.62 µm and 0.52 µm for the first and second centrifugation, respectively. The pellets after the second centrifugation were resuspended in UPW by agitation for 30 min in order to obtain colloidal suspension of 0.2 - 1 µm. The supernatants were also gently pipetted out and represented the fraction smaller than 0.2 µm.

For the four protocols ("a" through "d"), an aliquot of obtained suspension (fraction smaller than 1 µm) was passed through a 0.2-µm filter.

All filtrations at 2.7 µm and 1 µm were conducted with glass microfiber (VWR), which features a higher chemical resistance, pH resistance and biological inertia, and at 0.2 µm with a cellulose

nitrate membrane (Whatman). All centrifugations were performed using both a centrifuge (Thermo Scientific, Multifuge X3 FR) and a rotor (Thermo Scientific, FIBERLite F14-6x250LE). All experiments were run in triplicate.

Protocol "d" (combining centrifugation at 272 g and filtration at 1 µm, see Fig. 1) was selected for investigating the various sediment storage modes (wet, air-dried, oven-dried at 40°C, freeze-dried).

3. Colloid characterization

3.1. Colloid concentration and size distribution

The quantity of colloids was determined by gravimetric method. The filtrates at 1.0 µm (protocols "a" to "d") and suspension 0.2 - 1 µm (protocol "e") were passed through a 0.2-µm filter to retain the large colloidal fraction (0.2 - 1 µm), and the filters were oven-dried at 30°C until the mass remained unchanged. The colloidal concentration was quantified as a dry mass of colloid divided by the dry mass of sediment ($w_{DW\text{-}Colloid}/w_{DW\text{-}Sed}$). The particle size distribution of colloids was determined based on a dynamic light scattering technique using ZetaSizer NanoZS (Malvern) on the 0 - 1 µm (protocols "a" to "d") and 0.2 - 1 µm (protocol "e") suspensions. The material refraction index was set at 0.18 and the material absorption equaled 0.001. The angle of measurement was 173° backscatter; measurements started with a 120-second equilibration, followed by three measurements with an automatic selection of running times and optimal measurement position. The size distribution was presented according to number-based DLS data.

3.2. Chemical analysis for TP, Fe, Al, Mn, Ca, Mg, TOC

All chemical analyses were conducted on two fractions: 0 - 1 µm and 0 - 0.2 µm. The 0.2 - 1 µm fraction was determined by the difference between these two fractions across all separation methods, except for protocol "e" since the resuspended solution had already presented colloids sized 0.2 - 1 µm.

Total organic carbon (TOC) was measured using a TOC analyzer (Analytik Jena, multi N/C 2100S) with an LQ of 1 mg C/L. The organic content analysis was carried out with onboard magnetic stirring in order to avoid colloid aggregation and decantation.

Measurements of Fe, Al, Mn, Ca and Mg contents were recorded using MP-AES (Agilent, MP 4100). The LQ were: 30 µg/L ,20 µg/L, 7 µg/L, 12 µg/L and 1 µg/L, respectively. For the fraction smaller than 1 µm, prior to analysis the samples were acid digested with *aqua regia*, as presented in Method 3015a (US EPA, 2007) using a microwave digestion system (Anton Paar, Multiwave GO).

Total released phosphorus (TP) was analyzed after persulfate digestion according to Method 365.1 (US EPA, 1993). This method converts all forms of P into orthophosphate by autoclaving at 121°C for 30 minutes with ammonium persulfate and sulfuric acid. The content of digested orthophosphate, or dissolved inorganic phosphorus (DIP), was then measured by means of spectrophotometry using ammonium molybdate and antimony potassium tartrate, according to the method described by Murphy and Riley (1962). The amount of DIP was determined by the absorbance of molybdenum blue P, in conjunction with a UV-visible spectrophotometer at 880 nm (Agilent 8453 UV-visible spectrometer), using 1-cm cuvettes. Results were expressed in mg P/L. The limit of quantification (LQ) for this method is 0.01 mg P/L.

Four fractions of P could be determined: water-mobilizable P (P_{WM}: TP in the fraction smaller than 1 µm), large colloidal P (TP content in the 0.2 - 1 µm fraction, as identified by subtracting $TP_{< 0.2\ \mu m}$ from P_{WM}), small colloidal P (TP in the fraction smaller than 0.2 µm minus the dissolved P, as found by subtracting $DIP_{< 0.2\ \mu m}$ from $TP_{< 0.2\ \mu m}$), and dissolved P (evaluated by DIP in the fraction smaller than 0.2 µm). By this fractionation step, the small colloidal P covers P-colloids less than 0.2 µm, whereas large-colloidal P includes P-colloids from 0.2 to 1 µm.

4. Statistical analysis

A one-way analysis of variance (ANOVA) and two-tail t-test were used to analyze the significance of the differences between colloid separation methods and sediment storage modes at a 0.05 level of significance. The possible correlation between colloidal P and other colloidal elements was measured by means of the Pearson correlation coefficient R^2. All statistical analyses were run on Microsoft Excel, enhanced with Analysis ToolPak, XLSTAT and XL Toolbox NG.

RESULTS AND DISCUSSION

1. Separation protocols

1.1. Effects on the quantity of separated colloids and their size distribution

The mass of water-mobilizable colloids (0.2 - 1 µm) obtained according to five separation protocols is presented in mg colloid/$g_{DW\text{-}Sed}$ of sediment (Fig. 2). The colloid quantity varied between 5.4 ± 0.6 mg/$g_{DW\text{-}Sed}$ for direct filtration (protocol "a") and 21.2 ± 1.5 mg/$g_{DW\text{-}Sed}$ for successive centrifugation (protocol "e"), which corresponds to a factor of 4 across the tested assays.

When comparing protocol "a" with pre-separation filtration protocols "b" through "d", the introduction of a pre-separation step by filtration or centrifugation prior to filtration at 1 µm induced an increase of 1.5 to 2 times the mass of obtained colloids (from 7.3 ± 0.2 to 14.7 ± 0.4 mg/$g_{DW\text{-}Sed}$) relative to direct filtration at 1 µm (5.4 ± 0.6 mg/$g_{DW\text{-}Sed}$). The lower mass of colloids obtained by direct filtration, compared to "pre-treated" separation methods, is typically associated with membrane fouling, which decreases the flow rate due to an accumulation of particles at the surface (cake layer formation) or inside the membrane pores (Speth *et al.*, 2000; Gimbert *et al.*, 2005; Tang *et al.*, 2009). Cake layer formation is driven by both particle diameter and filter porosity with larger flocs/particles creating a thicker cake (Shirazi *et al.*, 2010). Introduction of the pre-separation step therefore helped reduce the deposition of coarser particles and resulted in an increase of colloid quantity passing through the 1-µm membrane. The decantation carried out prior to filtration in protocol "a" was insufficient to limit this phenomenon. However, the quantity of isolated colloids could also be decreased by colloid interaction with the filter or by attachment to larger particles retained by the membrane during filtration or aggregation to larger floc (Buffle and Leppard, 1995a; Stumm and Morgan, 1995). These interactions are not well understood, and more studies are needed to reveal the complex interactions taking place between colloid and membrane.

Application of a pre-centrifugation step (protocols "c" and "d") showed lower colloid recovery when compared with protocol "b" (pre-filtration at 2.7 µm), 10.5 ± 0.5 and 7.3 ± 0.2 against 14.7 ± 0.4 mg/$g_{DW\text{-}Sed}$, respectively. The mass of colloids further decreased by approximately 30% as the centrifugal force increased from 68 g (protocol "c") to 272 g (protocol "d") yet remained at least 1.4 times higher than direct filtration (protocol "a"). Separation by centrifugation could bring particles into closer contact and enhance aggregate formation (Vauthier *et al.*, 2008). An increase in

centrifugal force likely resulted in greater colloid collision and aggregation. Colloidal aggregates larger than 1 µm would be eventually separated in the subsequent filtration and could explain the lower mass observed in pre-centrifugation protocols. However, aggregate formation upon pre-centrifugation cannot be demonstrated in this study since no significant size discrimination for large colloids in the colloidal fraction (0.2 - 1 µm) were observed between two centrifugal speeds; moreover, for large aggregates, the size distribution of the particle fraction (i.e. above 1 µm) was not recorded herein. Although pre-centrifugation induced important mass loss of recovered colloids in subsequent filtrations compared to the successive filtration protocol, pre-centrifugation did remain a good solution for overcoming membrane clogging during direct filtration without any significant change in size distribution.

For successive centrifugation without filtration at 0.2 µm (protocol "e"), the colloid quantity was considerably higher than for the other protocols (by a factor ranging from 1.4 to 5), and the size distribution of obtained colloids revealed the presence of particles larger than 1,000 nm (Fig. 3). Meanwhile, the expected size was between 200 and 1,000 nm. During two successive centrifugations, the first aimed to remove particles larger than 1 µm and the second to separate colloidal from the conventional "dissolved fraction" at 0.2 µm. The appearance of particles larger than 1 µm after two successive centrifugations could be ascribed to an incomplete separation, caused by the heterogeneity of particle density and/or colloid aggregation/flocculation under high centrifugal forces. Particle density has an important role on the cut-off of colloidal particles separated by centrifugation using Stoke's law. The particles with lower density (for example organic particles) travel at a lower rate and at some point, will be separated from particles with higher density. Therefore, organic matter dominated particles would give a larger size cut-off than the particles dominated by minerals when subjected to the same centrifugation procedures (Klitzke *et al.*, 2012). According to our calculation, at the centrifugation speed of 272 g and 680 g and considering density of 1.2 g/cm^3 (for organic particles), the size of separated colloids was estimated to be 2.62 µm and 0.52 µm, respectively. The presence of particles larger than 1000 nm (Fig. 3) is a hint for presence of organic colloids. Moreover, as shown in figures 5a and 5b, the major component of separated colloids was organic carbon (9-12%). Thus, the colloids separated from studied sediment contained high amount of organic matter (estimated as 15-21% by a factor of 1.72 of total organic carbon). The incomplete separation of colloids during successive centrifugation (protocol "e") and associated higher size cut-off of separated colloids could be related colloid composition (with high organic content).

On the other hand, high density of colloids could favor colloid assemblies. Aggregation/flocculation may occur in the pellets or through colloid collision/agglomeration within supernatant (Salim and Cooksey, 1981; Baalousha, 2009; Maria *et al.*, 2020) to form large aggregates/flocs. In general, the supernatant obtained from the first supernatant could contain particles, colloidal and dissolved fractions.

When considering incomplete separation and aggregation with respect to the second-centrifuged supernatant, the presence of colloids larger than 0.2 µm could be expected even after the second centrifugation step. This has been confirmed by means of a size analysis of the fraction assumed to be smaller than 0.2 µm, in which 19% ± 15% of particles were in the range of greater than 200 nm for successive centrifugations, compared to 6% ± 3% for the other protocols (Fig. S1). Nevertheless, the presence of larger particles due to this incomplete separation has notably increased the expected mass of colloids (Fig. 2) and can lead to overestimating the colloidal fraction. This finding

highlights the importance of considering not only the weight of extracted colloids but also their size distribution.

The large colloidal and dissolved fractions separated by all tested protocols contained high amounts of organic, Al and Fe and lower contents of Ca, Mg and Mn (Fig. 5a and 5b). Chemical composition of extracted colloids and dissolved fractions was related to composition of sediment (Table 2) which was related to local geological context (mainly granitic). As shown in figures 4 and 5a, the masses of P, OC, Fe, Al, Ca, Mn and Mg recovered in fraction lower than 1 µm were respectively: from 30.1 ± 2.1 to 85.3 ± 7.8 µg $P/g_{DW\text{-}Sed}$, 1330 ± 160 to 3500 ± 400 µg $C/g_{DW\text{-}Sed}$, 430 ± 30 to 1300 ± 100 µg $Fe/g_{DW\text{-}Sed}$, 750 ± 70 to 2500 ± 200 µg $Al/g_{DW\text{-}Sed}$, 460 ± 30 to 730 ± 90 µg $Ca/g_{DW\text{-}Sed}$, 8.8 ± 0.1 to 21.9 ± 0.2 µg $Mn/g_{DW\text{-}Sed}$ and 115 ± 5 to 250 ± 2 µg $Mg/g_{DW\text{-}Sed}$. Water-mobilizable fraction (below 1 µm) represented 2.1 – 6%, 0.7 – 1.8%, 0.5 – 1.6%, 0.5 – 1.9%, 5.4 – 8.6%, 0.5 – 1.5% and 0.7 – 1.4% of total sedimentary P, OC, Fe, Al, Ca, Mn and Mg contents. The percentages were obtained under experimental gentle agitation with UPW and probably did not represent all the mobilizable P-colloids in natural system. The large colloids (0.2 – 1 µm) represented 67 – 90%, 50 – 67%, 76 – 94%, 87 – 98%, 61 – 67%, 54 – 98% and 62 – 72% of P, OC, Fe, Al, Ca, Mn and Mg contents in water-mobilizable fraction (below 1 µm).

It is important to highlight that higher release of OC in large colloids (0.2 – 1 µm) by successive centrifugation protocol were concomitating with higher release of Al, Fe, Mg and P. In fraction below 0.2 µm, this release of OC was with Al, Ca, Fe, Mg, P and Mn. This suggesting the remaining colloids after centrifugation could be organo-mineral colloids.

Furthermore, there are difficulties in comparison potential of sediment to mobilize colloids with other terrestrial systems as most of the studies presented colloid concentration by volume of extract. Dissimilarities between the method used to extract and separate colloid, S/L ratio and cut-off size for colloidal fraction do not allow straight comparison. However, to some extents, the estimation of colloidal stock in sediment can be relatively determined. For example, Sinaj *et al.* (1998) showed colloid concentrations of 0.26 – 1.32 $g/kg_{DW\text{-}Soil}$ in Ap horizon soils for fraction 0.025 – 0.45 µm separated by centrifugation combining filtration and with similar S/L ratio of 1/10 to present work. Our sediment showed a colloid concentration of 7.29 – 10.52 $g/kg_{DW–Sed}$ for fraction 0.2 – 1 µm by similar separation protocol (protocols “d” and “c”). Hence, the amount of colloids in reservoir sediment is 7 – 10 times higher than in soil reported by Sinaj *et al.* (1998). This drastic variation might indicate the higher potential of reservoir sediment to release colloids than in soil. However, it should be noted a different in cut-off size can derive incomparable data; as taken into the work of Yan *et al.* (2017), large colloids (0.45 – 1 µm) contributed lower proportion (approximately 38 %) than small colloidal in total soil colloids (0.1 – 1 µm) separated by successive centrifugation.

1.2. Effects on water-mobilizable phosphorus

The concentrations of water-mobilizable phosphorus (P_{WM}) obtained from five separation protocols are presented in three size-based forms: DIP; “small colloidal P” containing colloids sized below 200 nm; and “large colloidal P” containing P-colloids sized 0.2 µm - 1 µm. The concentration of P_{WM} is presented in µg of P per g_{DW} of sediment (Fig. 4).

The release of P_{WM} varied between 30.1 ± 1.6 (direct filtration) and 85.3 ± 9.6 µg $P/g_{DW\text{-}Sed}$ (successive centrifugations) in proportion with the mass of colloids released from the sediment (R^2 = 0.88). The P_{WM} distribution between dissolved, small and large colloidal fractions was relatively

similar for all tested separation protocols, except successive centrifugations (protocol "e"). Generally, P_{WM} presented mainly in large colloids (> 0.2 µm; 67% - 90%). The lowest quantity of large P-colloids was observed after direct filtration (protocol "a", 23.1 ± 2.0 µg/$g_{DW\text{-}Sed}$), while the highest amount was obtained after successive centrifugations (protocol "e", 57.1 ± 7.5 µg/$g_{DW\text{-}Sed}$) and varied proportionally to the mass of P_{WM}. The quantities of small colloidal P were less than 1.3 ± 0.6 µg/$g_{DW\text{-}Sed}$ and contributed up to 4% of P_{WM} for the separation protocols using filtration (protocols "a" to "d"). As opposed to other protocols, namely the successive centrifugations protocol, a significant contribution of small P-colloid was observed (30% ± 3%). An increasing amount of small colloidal P in successive centrifugations might be due to the remaining large colloids due to incomplete separation in second-centrifuged supernatant. These colloids were organic or organo-mineral considering their chemical composition (Fig. 5b).

The quantities of dissolved P were not strongly impacted by any of the separation protocols, with an average of 4.5 ± 1.1 µg/$g_{DW\text{-}Sed}$, constituting 11% ± 6% of P_{WM} and 0.3% ± 0.1% of total sedimentary P. As such, the total colloidal P in both the small and large colloids accounted for 1.7% - 5.8% of total sedimentary P, which far exceeds dissolved P, thus highlighting the major contribution of P-colloids, beyond the focus on truly dissolved P.

In comparison to studies on soil samples, in the present work, the contribution of colloidal P in fraction lower than 1 µm represented 81 – 93 %, which is relatively higher than the contribution of colloidal P extracted from soils. For example, for agricultural soil, Liang *et al.* (2010) found that 25.5 % of total P in fraction below 1 µm came from colloidal form and Liu *et al.* (2014) reported proportions of 55.2 – 80.9 % for colloidal fraction between 0.02 – 1 µm. In study performed on wetland soils, Gu *et al.* (2018) found up to 70 % of nano and small colloidal P contributed to $TP_{< 0.45\ \mu m}$ but in different size range 5 kDa – 0.45 µm. Even though, the important proportions of the colloidal P found in other studies and in our study highlight the significant contribution of this fraction to the potential mobilization of P from sediment to the water column and the interest to improve knowledge about this fraction.

1.3. Effects on the chemical composition of large colloids (0.2 -1 µm)

Figure 5c presents the elemental composition of P, OC, Fe, Al, Ca, Mn and Mg in separated large colloids. The P concentration obtained by successive centrifugations (protocol "e") equaled 2.7 ± 0.5 mg/$g_{DW\text{-}Colloid}$, which was similar to the successive filtrations (protocol "b", 3.14 ± 0.12 mg/$g_{DW\text{-}Colloid}$) and low-speed centrifugation-filtration (protocol "c", 3.6 ± 0.3 mg/$g_{DW\text{-}Colloid}$). However, these concentrations were less than those in colloids separated by direct filtration (protocol "a") and high-speed centrifugation-filtration (protocol "d"), with 4.4 ± 0.6 and 4.4 ± 0.4 mg/$g_{DW\text{-}Colloid}$, respectively. The concentrations of Ca, Mn and Mg in large colloids also varied across the separation protocols, with higher values being observed for protocols "a" and "d" (i.e. 54.2 ± 7.5 and 47.5 ± 4.4 mg Ca/$g_{DW\text{-}Colloid}$, 1.6 ± 0.2 and 1.8 ± 0.5 mg Mn/$g_{DW\text{-}Colloid}$, 13.6 ± 0.9 and 10.1 ± 0.2 mg Mg/$g_{DW\text{-}Colloid}$, respectively. Therefore, the higher concentrations of P for protocol "a" and "d" can be linked to higher in concentrations of Ca, Mn and Mg. On the other hand, the difference in separation protocols seems to exert no influence on the concentrations of OC, Fe and Al in large colloids (one-way ANOVA: $p > 0.05$ for OC and Fe, t-test for each pair of means for Al), with average values of 105 ± 6, 56.5 ± 7.0 and 114 ± 13 mg/$g_{DW\text{-}Colloid}$, respectively. For P, Ca, Mn and Mg elements, the low concentrations in large colloids after separation by means of successive centrifugations, in spite of the higher dry mass, may be caused by dilution due to the presence of large particles resulting from

incomplete separation, because colloids have higher specific surface area than particles (Biermann, 1996).

On the whole, the successive centrifugations should be considered with caution since this technique introduces a high probability of incomplete separation, which in turn can lead to overestimating quantity and underestimating quality of the colloidal fraction. Special attention should be paid to organic rich sediment which could induce higher error in size separation by this method and overestimation of colloid mass and size. Among the four separation protocols using filtration, successive filtrations provided the highest recovery in colloid quantity, whereas high-speed centrifugation and filtration delivered lower colloid quantity, though with colloids richer in P content. In the next section, as regards the role of P in the aquatic environment, an assessment of several sediment storage modes will be conducted from the colloid separated by high-speed centrifugation and filtration (protocol "d") in order to obtain colloids with elevated P contents.

2. Sediment storages

2.1. Effects on the quantity of extracted colloids and their size distribution

The mass of large colloids (0.2 - 1 µm) and the size distribution of the fraction smaller than 1 µm are presented in Figures 6 and 7, respectively. From here, the wet sediment will be considered as a reference when assessing the influence of various sediment drying on the quantity and quality of water-mobilizable colloids obtained according to protocol "d" (high-speed centrifugation and filtration, Fig. 1).

As displayed in Figure 6, various modes of sediment storage prior to colloid extraction performed strong influence on the quantity of colloids actually yielded. The mass of colloids (0.2 - 1 µm) obtained from the wet sediment was 7.3 ± 0.2 mg/$g_{DW\text{-}Sed}$, as decreased by 18% and 28% after sediment drying at 20°C and 40°C, respectively, and by 82% after freeze-drying. Sediment drying had also exerted an impact on the size distribution of water-mobilizable colloids (Fig. 7). In the first part of this study, we showed that when the "d" protocol was used for colloid separation, 94% of the released colloids were sized smaller than 450 nm; also, colloids sized 0 - 50 nm did not appear in extracted supernatant from the wet sediment. We noted that even after sediment drying and rewetting, this fraction remained undetectable. We did however observe an impact of sediment drying on the 50 - 100 nm, 100 - 220 nm and 220 - 450 nm fractions. The percentages of colloids sized 50 - 100 nm declined significantly, i.e. from 29% ± 1% in wet sediment to less than 5% in dried sediment regardless of the drying mode, whereas the percentage of the 100 - 450 nm fraction increased from 65% ± 14% for wet sediment to 95% ± 2% for dried sediment.

The observed decrease in colloidal mass and the change in colloidal size distribution may be due to two phenomena: (i) an increase in the hydrophobicity and/or (ii) an aggregation occurring during the evaporation of water by desiccation and freeze-drying. The first phenomenon concerns an increase in water repellency on solid surfaces during drying, which implies an increase in the hydrophobicity of solid phases (Dekker *et al.,* 2001; Klitzke and Lang, 2007). The intensification of hydrophobicity involves the retention of colloidal particles on the surface of solids, and thus affects their dispersibility after rewetting (Klitzke and Lang, 2007). It is also postulated that colloids become more hydrophobic during drying and become less mobile after rewetting (Klitzke and Lang, 2007; Wan and Wilson, 1994). Another possible explanation for the decrease in colloid recovery after drying is aggregation. During water elimination, the cohesive forces of capillary-bound water increase with the decrease in pore water pressure and thus increase the effectiveness of bridging and cementing materials (Munkholm and Kay, 2002). Especially during freeze-drying, through the sublimation of ice

crystals, the water molecular layers in electrical double layers are limited, which in turn enhances short-range attractive forces and accelerates both colloid-colloid and colloid-particle flocculation (Dagesse, 2011). Moreover, the duration of drying process plays an important role in colloid mobility (Majdalani *et al.*, 2008; Mohanty *et al.*, 2015). Drying would initially enhance colloid release because during the early period of drying, pore walls are broken under capillary stress that favor colloids generation. However, after a critical period of 2.5 or 9 - 11 days, according to cases cited in Mohanty *et al.* (2015) and Majdalani *et al.* (2008), the quantity of mobilized colloid decreases. This phenomenon was explained by the precipitation of salts and minerals in pore water during evaporation, which according to the authors serves to bind colloids and prevent their mobilization during rewetting (Majdalani *et al.*, 2008). Moreover, further drying can lead to the hydraulic disconnection of previously saturated pores and might limit the diffusive transport of colloids from matrix to solution (Mohanty *et al.*, 2015). It is therefore possible that in our study the important decrease in mass of large colloids was associated with the precipitation of dissolved Fe and Al during drying (2 weeks for 20°C-dried sediment, 5 days for 40°C-dried sediment and 4 days for freeze-dried sediment). As shown in Figure 8b, in most cases, a lower release of Fe and Al in the fraction below 0.2 µm (generally defined as dissolved) was observed when using dried sediments as compared to wet ones. The release of Fe from wet sediment to the fraction smaller than 0.2 µm amounted to 78 ± 22 $\mu g/g_{DW\text{-}Sed}$, dropping to 37 ± 9 $\mu g/g_{DW\text{-}Sed}$, 25 ± 22 $\mu g/g_{DW\text{-}Sed}$ and 14 ± 2 $\mu g/g_{DW\text{-}Sed}$ ($p < 0.05$) in the experiments carried out on sediments dried at 20°C, 40°C and by freezing, respectively. For Al, the release from wet sediment was 53 ± 14 $\mu g/g_{DW\text{-}Sed}$ and significantly decreased after 40°C and freeze-drying to reach 27 ± 4 $\mu g/g_{DW\text{-}Sed}$ and 4.6 ± 0.6 $\mu g/g_{DW\text{-}Sed}$ respectively ($p < 0.05$). The drying of sediment at 20°C seems to exert no impact on the amount of dissolved Al. The lower release of dissolved Fe for all dry modes and Al for 40°C-dried and freeze-dried sediments suggested that Fe and Al precipitation may have played a role in the formation of cement bridges binding the colloids to one another and/or the colloids with sediment particles; moreover, the dissolved Fe and Al could interact with large colloids and promote their aggregation. Thus, colloids bound to sediment particles (by cementation or increased solid phases/colloid hydrophobicity) and/or contained in the aggregates larger than 1 µm were eliminated during the extraction and/or separation steps or else were not mobilized after rewetting. As shown in Figure 8a, a portion of large Al-, Fe- and Ca-colloids were impacted by the processes described above at an intensity varying by sediment drying mode. The lowest release of large Fe- and Al-colloids occurred after freeze-drying, with quantities of 80 ± 30 and 160 ± 40 $\mu g/g_{DW\text{-}Sed}$ respectively, corresponding to 0.11% and 0.12% of total sedimentary Fe and Al, against 480 ± 110 and 940 ± 150 $\mu g/g_{DW\text{-}Sed}$ respectively (corresponding to 0.61% and 0.69% of total sedimentary contents) found in colloids separated from wet sediment. The Ca quantities in large colloids were similar across three sediment drying modes ($p > 0.05$), with an average value of 160 ± 20 $\mu g/g_{DW\text{-}Sed}$ which were two-times lower than for the wet one, and composed of 1.8% ± 0.2% of total sedimentary Ca. In contrast, it seems that large water-mobilizable OC-, Mn- and Mg-colloids were not impacted by sediment drying at 20°C and 40°C, but only by freeze-drying. Their colloid quantities in 20°C- and 40°C-dried sediments were: 870 ± 60, 12 ± 2 and 61 ± 4 $\mu g/g_{DW\text{-}Sed}$, respectively, representing 0.45%, 0.82% and 0.36% of total sedimentary OC, Mn and Mg. These quantities of OC, Mn and Mg in large colloids dropped to 290 ± 30, 0.6 ± 0.6 and zero $\mu g/g_{DW\text{-}Sed}$ when the sediment was freeze-dried, thus representing lower proportions in total sedimentary contents (0.15% and 0.04% for OC and Mn). Several studies have reported an increase in the solubility of organic matter following drying, as attributed to microbial lysis and the disruption of organic matter coatings on mineral particles (e.g. Bartlett and James, 1980; Turner *et al.*, 2003). A greater release of dissolved and/or colloidal OC would thus be expected, but as presented in Figures 8a and 8b, differences in the OC pool in the 0 - 0.2 µm and 0.2 - 1 µm fractions remained relatively

small (except for large OC colloids in the freeze-drying assay) and lied within the error expected for replicate analyses. This finding indicates that air-drying and oven-drying cause no systematic changes in OC release; furthermore, if the disruption of organic matter coatings on the mineral particles occurred during drying pretreatment, then this step shall produce OC in the fraction larger than 1 µm and hence was not evaluated herein. Our results indicate the preferential immobilization of inorganic colloids during air and oven drying comparing to organic colloids, which underline their different mobility after drying. This result is consistent with the observations reported by Klitzke and Lang, (2007) suggesting that the dispersibility of colloids after drying depends on their composition and that organic colloids are more mobile than organo-minerals colloids. In addition, we observed a decreasing release of large OC colloids in freeze-dried sediment, most likely due to the formation of larger particles (or more hydrophobic) and their retention during the extraction and/or filtration step. Freeze-drying is a common method employed to avoid microbial and chemical degradation in samples (Sun *et al.*, 2015; Weißbecker *et al.*, 2017; Wu *et al.*, 2018). However, the use of freeze-dried sediment instead of fresh sediment can result in a significant underestimation of water-mobilizable OC, Fe, Al, Ca, Mn and Mg.

2.2. Effects on water-mobilizable phosphorus

The variation in P_{WM} quantities induced by the different sediment drying modes is presented in Figure 9, in comparison to the reference (wet sediment). We observed that P_{WM} recovery during colloid extraction was significantly altered by the freeze-drying pretreatment step. The amounts of P_{WM} extracted from wet, 20°C- and 40°C-dried sediments were comparable, at 36 ± 3 µg/$g_{DW\text{-}Sed}$, whereas with freeze-drying, P_{WM} recovery decreased by a quarter compared to the initial value, reaching 27 ± 1 µg/$g_{DW\text{-}Sed}$. A lower release of P_{WM} from freeze-dried sediment is primarily due to the decrease in large P-colloids and probably due to the same processes explaining colloidal OC retention (see previous section). On the other hand, the sediment drying pretreatment step led to an alteration in the size-based forms of P_{WM}, regardless of drying mode, by increasing small-sized colloidal P from 0.35 ± 0.17 µg/g $g_{DW\text{-}Sed}$ for wet sediment to reach 2.5 ± 0.7 µg/$g_{DW\text{-}Sed}$ for the 20°C-dried and 4.2 ± 0.7 µg/$g_{DW\text{-}Sed}$ for the 40°C-dried and freeze-dried modes. The small-sized P-colloids only contributed 1.0% ± 0.4% of total P_{WM} in wet sediment, while this P fraction rose to 8% ± 3% for 20°C-dried, 11% ± 3% for 40°C-dried and 16% ± 2% for freeze-dried sediments. Thus, air-, oven- and freeze-drying generated small-sized colloidal P, probably in the range of 100 - 200 nm, in accordance with an increase in the 100 - 220 nm sized fraction (Fig. 7). In sediments, P can be associated with the organic fraction and with primary and/or secondary minerals, which are mostly composed of Fe, Mn and Al oxi-hydroxides and Ca phases (Pettersson *et al.*, 1988). According to the literature, drying may induce the solubilization of small-sized P-colloids because of microbial cell lysis and/or organic matter solubilization through disrupting the mineral particle organic coating (Turner *et al.*, 2003). However, as indicated in Figures 8a and 8b, the expected increase in OC release was not observed for dried sediments. A greater release of Ca and Mg in the 0 - 0.2 µm fraction from all dried sediments (Fig. 8b) suggests that small P-colloids released from dried sediments originated rather from inorganic particles and were or still are associated or generated along with Ca and/or Mg. It is also possible that a portion of small-sized P colloids was produced by the (co)precipitation of DIP during drying. As shown in Figure 9, the amount of dissolved P decreased from 4.7 ± 0.1 µg/$g_{DW\text{-}Sed}$ for wet sediment to 3.0 ± 0.1 µg/$g_{DW\text{-}Sed}$, 2.0 ± 0.4 and 2.6 ± 0.2 for 40°C-dried, 20°C-dried and freeze-dried sediments, respectively. Thus, across all sediment storage modes, the principal fraction of P_{WM} came from large-sized colloidal P (i.e. larger than 0.2 µm), which varied from 75% ± 4% to 87% ± 8% of P_{WM}, against 5% ± 1% to 13% ± 1% for truly dissolved P. Therefore, the large-size

colloidal fraction plays a substantial role in the mobilization of P from sediment to aqueous phase. The P_{WM} recovered from wet and dried sediments represented 2.4 ± 0.3% of total sedimentary P.

2.3. Effect on chemical composition of colloids

The total mass of recovered elements (P, OC, Al, Fe, Ca, Mg and Mn) in 0.2 – 1 µm fraction represent 37 ± 2% of the mass of large water-mobilizable colloids released from wet, 20°C-dried and 40°C-dried sediments and 51% of the mass of colloids released from freeze-dried sediments. Taking into account the local geological context of Champsanglard reservoir (i.e. mainly granitic (Rapin *et al.*, 2019a)), the missing mass is probably due to Si, Na, K and other elements (not evaluated in this study). When considering the measured elements, we can conclude that the major components of large colloids mobilized from wet sediment were: Al (128 ± 18 mg $Al/g_{DW\text{-}Colloid}$) and OC (123 ± 19 mg $C/g_{DW\text{-}Colloid}$), followed by Fe (67 ± 13 mg $Fe/g_{DW\text{-}Colloid}$) and Ca (48± 5 mg $Ca/g_{DW\text{-}Colloid}$), with a smaller share ascribed to Mg (10.1 ± 0.2 mg $Mg/g_{DW\text{-}Colloid}$), P (4.4 ± 0.3 mg $P/g_{DW\text{-}Colloid}$) and Mn (1.8 ± 0.5 mg $Mn/g_{DW\text{-}Colloid}$). Sediment drying affected differently the release of individual elements in colloidal form, so the chemical composition of recovered colloids depended on the sediment drying mode. For example, sediment drying at 20°C (compared to wet sediment) favored the release of colloidal OC and lowered the release of colloidal Ca, whereas drying at 40°C favored the release of colloidal P (1.5 times higher) and decreased the release of colloidal Ca. Freeze-drying drastically favored the release of colloidal P (3 times higher), Ca (2.6 times) and OC (1.5 times) while decreasing by a factor of 5 the release of colloidal Mn and by 10 the release of Mg (Fig. 8c). Freeze-drying resulted in releasing the lowest quantity of colloids compared to wet and 20°C-dried or 40°C-dried sediments. However, it is noticeably that freeze-drying led to enriching large colloids by P and Ca.

Conclusion and Recommendations

Based on our experimental data, it can be concluded that diversification in applied separation and sample storage induce significant variation in quantity and physicochemical characteristics of recovered colloids. Apart from confirmation that loss of colloids by membrane fouling during filtration can be improved by introducing a pre-separation step via filtration at a greater pore size or with centrifugation. The successive centrifugations, a usual alternative protocol for filtration, also showed obstacle in size accuracy. The incomplete separation between colloids and particles under centrifugal forces in our cases highlights the participation of colloid aggregation/flocculation and of heterogeneity in particle density. The latter one refers to difference in density of organic and inorganic particles, hence, chemical composition of sediment strongly affected the colloid separation. Those sediments rich in organic matter like our case could result in overestimation of colloid quantity obtained with these successive centrifugations.

As opposed to the impact of varying separation protocols on colloid quantity, changing the sediment storage modes (drying at 20°C, at 40°C and by lyophilization) led to a critical modification in both quantity and characteristics of recovered colloids (size and chemical composition). The drying of sediment decreases colloids quantity and altered their size distribution by increasing small/intermediate-sized colloids and decreasing nano-colloids. Furthermore, organic colloids behave differently to mineral-rich colloids upon drying. Mineral or organo-mineral colloids could be prone to immobilization in sediment structure after drying than organic colloids due to cementation and increase of sediment/colloid hydrophobicity. Therefore, the common storage by drying at 20°C is not appropriate for sediment's colloid characterization.

From these considerations, effect of colloid separation and sample storage on colloid recovery are specific to sample characteristics and experimental approaches. Dissimilarities in colloid quantity and characteristics are at a factor up to 40 depending on sample storages and up to 26 according to colloid separation protocols. Hence, this may drastically alter the interpretation of how sedimentary colloids behave *in situ*. No standard methods currently exist for either sediment storage or colloid separation prior to the quantification of water-mobilizable colloids. Straight comparison of colloid composition in sediment or soils cannot be done unless special care should be paid to solid composition, solid storage and colloid separation protocol.

Based on our findings, we recommend working with fresh moist sediment and to elude the use of successive centrifugation protocol for colloid separation.

Apart from an insight to the heterogeneity between colloid extraction protocols, this study also shed a light on the strong potential of bottom sediment to release colloids and associated contaminants/nutrients to surface water which has been rarely investigated in dam reservoir context. To some extent, our data can enrich current knowledge on mobility of colloidal P in reservoir context. Dam reservoir sediment exhibited a relatively high potential of water-mobilizable colloids, with over 5.4 $g/kg_{DW\text{-}Sed}$ and those colloids could deliver approximately more than 25 mg $P/kg_{DW\text{-}Sed}$.

Acknowledgments

The authors would like to thank France's Nouvelle-Aquitaine Regional Council, the EDF electric utility company and the "Dam and Water Quality" Chair of Excellence with the "University of Limoges Partnership Foundation" for financially supporting this research work.

References

Baalousha, M., Stolpe, B., & Lead, J. R. (2011). Flow field-flow fractionation for the analysis and characterization of natural colloids and manufactured nanoparticles in environmental systems: A critical review. *Journal of Chromatography A*, *1218*(27), 4078–4103. https://doi.org/10.1016/j.chroma.2011.04.063

Baalousha, M. (2009). Aggregation and disaggregation of iron oxide nanoparticles: Influence of particle concentration, pH and natural organic matter. *Science of The Total Environment*, *407*(6), 2093–2101. https://doi.org/10.1016/j.scitotenv.2008.11.022

Baken, S., Moens, C., van der Grift, B., & Smolders, E. (2016). Phosphate binding by natural iron-rich colloids in streams. *Water Research*, *98*, 326–333. https://doi.org/10.1016/j.watres.2016.04.032

Baken, S., Regelink, I. C., Comans, R. N. J., Smolders, E., & Koopmans, G. F. (2016). Iron-rich colloids as carriers of phosphorus in streams: A field-flow fractionation study. *Water Research*, *99*, 83–90. https://doi.org/10.1016/j.watres.2016.04.060

Bartlett, R., & James, B. (1980). Studying Dried, Stored Soil Samples—Some Pitfalls. *Soil Science Society of America Journal*, *44*(4), 721–724. https://doi.org/10.2136/sssaj1980.03615995004400040011x

Bergendahl, J., & Grasso, D. (1998). Colloid generation during batch leaching tests: Mechanics of disaggregation. *Colloids and Surfaces A: Physicochemical and Engineering Aspects*, *135*(1), 193–205. https://doi.org/10.1016/S0927-7757(97)00248-3

Biermann, C. J. (1996). 21—Colloid and Surface Chemistry. In C. J. Biermann (Ed.), *Handbook of Pulping and Papermaking (Second Edition)*, 421–437. Academic Press. https://doi.org/10.1016/B978-012097362-0/50025-X

Bradford, S. A., Yates, S. R., Bettahar, M., & Simunek, J. (2002). Physical factors affecting the transport and fate of colloids in saturated porous media: factors affecting the fate of colloids. *Water Resources Research*, *38*(12), 1327. https://doi.org/10.1029/2002WR001340

Buermann, Y., Du Preez, H. H., Steyn, G. J., Harmse, J. T., & Deacon, A. (1995). Suspended silt concentrations in the lower Olifants River (Mpumalanga) and the impact of silt releases from the Phalaborwa Barrage on water quality and fish survival. *Koedoe*, *38*(2), 11–34.

Buettner, S. W., Kramer, M. G., Chadwick, O. A., & Thompson, A. (2014). Mobilization of colloidal carbon during iron reduction in basaltic soils. *Geoderma*, *221–222*, 139–145. https://doi.org/10.1016/j.geoderma.2014.01.012

Buffle, J., & Leppard, G. G. (1995a). Characterization of Aquatic Colloids and Macromolecules. 1. Structure and Behavior of Colloidal Material. *Environmental Science & Technology, 29*(9), 2169-2175. https://pubs.acs.org/doi/abs/10.1021/es00009a004

Buffle, J., & Leppard, G. G. (1995b). Characterization of aquatic colloids and macromolecules. 2. Key role of physical structures on analytical results. *Environmental Science & Technology*, *29*(9), 2176–2184.

Cavaliere, E., & Homann, P. (2012). Elwha River Sediments: Phosphorus Characterization and Dynamics Under Diverse Environmental Conditions. *Northwest Science*, *86*(2), 95–107. https://doi.org/10.3955/046.086.0202

Cervi, E. C., Hudson, M., Rentschler, A., & Burton, G. A. (2019). Metal Toxicity During Short-Term Sediment Resuspension and Redeposition in a Tropical Reservoir. *Environmental Toxicology and Chemistry*, *38*(7), 1476–1485. https://doi.org/10.1002/etc.4434

Châtellier, X., Grybos, M., Abdelmoula, M., Kemner, K. M., Leppard, G. G., Mustin, C., West, M. M., & Paktunc, D. (2013). Immobilization of P by oxidation of Fe(II) ions leading to nanoparticle formation and aggregation. *Applied Geochemistry*, *35*, 325–339. https://doi.org/10.1016/j.apgeochem.2013.04.019

Chen, B., & Beckett, R. (2001). Development of SdFFF-ETAAS for characterizing soil and sediment colloids. *The Analyst*, *126*(9), 1588–1593. https://doi.org/10.1039/b102087k

Chittleborough, D. J., Hotchin, D. M., & Beckett, R. (1992). Sedimentation field-flow fractionation: a new technique for the fractionation of soil colloids. *Soil Science*, *153*(5), 341.

Corzo, A., Jiménez-Arias, J. L., Torres, E., García-Robledo, E., Lara, M., & Papaspyrou, S. (2018). Biogeochemical changes at the sediment–water interface during redox transitions in an acidic reservoir: Exchange of protons, acidity and electron donors and acceptors. *Biogeochemistry*, *139*(3), 241–260. https://doi.org/10.1007/s10533-018-0465-7

Cuss, C. W., Donner, M. W., Grant-Weaver, I., Noernberg, T., Pelletier, R., Sinnatamby, R. N., & Shotyk, W. (2018). Measuring the distribution of trace elements amongst dissolved colloidal species as a fingerprint for the contribution of tributaries to large boreal rivers. *Science of The Total Environment*, *642*, 1242–1251. https://doi.org/10.1016/j.scitotenv.2018.06.099

Dagesse, D. (2011). Effect of freeze-drying on soil aggregate stability. *Soil Science Society of America Journal*, *75*(6), 2111–2121.

Dai, M., Buesseler, K. O., Ripple, P., Andrews, J., Belastock, R. A., Gustafsson, Ö., & Moran, S. B. (1998). Evaluation of two cross-flow ultrafiltration membranes for isolating marine organic colloids. *Marine Chemistry*, *62*(1–2), 117–136.

Dekker, L. W., Doerr, S. H., Oostindie, K., Ziogas, A. K., & Ritsema, C. J. (2001). Water repellency and critical soil water content in a dune sand. *Soil Science Society of America Journal*, 65(6), 1667-1674. http://soil.scijournals.org/cgi/reprint/65/6/1667.pdf

Doucet, F. J., Maguire, L., & Lead, J. R. (2005). Assessment of cross-flow filtration for the size fractionation of freshwater colloids and particles. *Talanta*, *67*(1), 144–154. https://doi.org/10.1016/j.talanta.2005.02.026

Effler, S. W., & Matthews, D. A. (2004). Sediment resuspension and drawdown in a water supply reservoir. *Journal of the American Water Resources Association*, *40*(1), 251–264. https://doi.org/10.1111/j.1752-1688.2004.tb01023.x

Filstrup, C. T., & Lind, O. T. (2010). Sediment transport mechanisms influencing spatiotemporal resuspension patterns in a shallow, polymictic reservoir. *Lake and Reservoir Management*, *26*(2), 85–94. https://doi.org/10.1080/07438141.2010.490771

Gálvez, J. A., & Niell, F. X. (1992). Sediment resuspension in a monomictic eutrophic reservoir. *Hydrobilogia*, 133–141. https://doi.org/10.1007/BF00026206

Gautreau, E., Volatier, L., Nogaro, G., Gouze, E., & Mermillod-Blondin, F. (2020). The influence of bioturbation and water column oxygenation on nutrient recycling in reservoir sediments. *Hydrobiologia*, *847*(4), 1027–1040. https://doi.org/10.1007/s10750-019-04166-0

Gimbert, L. J., Haygarth, P. M., Beckett, R., & Worsfold, P. J. (2005). Comparison of Centrifugation and Filtration Techniques for the Size Fractionation of Colloidal Material in Soil Suspensions Using Sedimentation Field-Flow Fractionation. *Environmental Science & Technology*, *39*(6), 1731–1735. https://doi.org/10.1021/es049230u

749 Gimbert, L. J., Haygarth, P. M., Beckett, R., & Worsfold, P. J. (2006). The Influence of Sample
750 Preparation on Observed Particle Size Distributions for Contrasting Soil Suspensions using
751 Flow Field-Flow Fractionation. *Environmental Chemistry*, *3*(3), 184.
752 https://doi.org/10.1071/EN06029
753 Gottselig, N., Amelung, W., Kirchner, J. W., Bol, R., Eugster, W., Granger, S. J., Hernández-Crespo, C.,
754 Herrmann, F., Keizer, J. J., Korkiakoski, M., Laudon, H., Lehner, I., Löfgren, S., Lohila, A.,
755 Macleod, C. J. A., Mölder, M., Müller, C., Nasta, P., Nischwitz, V., … Klumpp, E. (2017).
756 Elemental Composition of Natural Nanoparticles and Fine Colloids in European Forest
757 Stream Waters and Their Role as Phosphorus Carriers: Colloids in European forest streams.
758 *Global Biogeochemical Cycles*, *31*(10), 1592–1607. https://doi.org/10.1002/2017GB005657
759 Gottselig, N., Nischwitz, V., Meyn, T., Amelung, W., Bol, R., Halle, C., Vereecken, H., Siemens, J., &
760 Klumpp, E. (2017). Phosphorus Binding to Nanoparticles and Colloids in Forest Stream
761 Waters. *Vadose Zone Journal*, *16*: 1-12 vzj2016.07.0064.
762 https://doi.org/10.2136/vzj2016.07.0064
763 Grolimund, D., Elimelech, M., Borkovec, M., Barmettler, K., Kretzschmar, R., & Sticher, H. (1998).
764 Transport of in Situ Mobilized Colloidal Particles in Packed Soil Columns. *Environmental*
765 *Science & Technology*, *32*(22), 3562–3569. https://doi.org/10.1021/es980356z
766 Gu, S., Gruau, G., Malique, F., Dupas, R., Petitjean, P., & Gascuel-Odoux, C. (2018). Drying/rewetting
767 cycles stimulate release of colloidal-bound phosphorus in riparian soils. *Geoderma*, *321*, 32–
768 41. https://doi.org/10.1016/j.geoderma.2018.01.015
769 Hahn, J., Opp, C., Evgrafova, A., Groll, M., Zitzer, N., & Laufenberg, G. (2018). Impacts of dam
770 draining on the mobility of heavy metals and arsenic in water and basin bottom sediments of
771 three studied dams in Germany. *Science of The Total Environment*, *640–641*, 1072–1081.
772 https://doi.org/10.1016/j.scitotenv.2018.05.295
773 Hart, Barry T., Douglas, G. B., Beckett, R., Van Put, A., & Van Grieken, R. E. (1993). Characterization of
774 colloidal and particulate matter transported by the Magela Creek system, northern Australia.
775 *Hydrological Processes*, *7*(1), 105–118.
776 Hassellov, M., Buesseler, K., Pike, S., & Dai, M. (2007). Application of cross-flow ultrafiltration for the
777 determination of colloidal abundances in suboxic ferrous-rich ground waters☆. *Science of*
778 *The Total Environment*, *372*(2–3), 636–644. https://doi.org/10.1016/j.scitotenv.2006.10.001
779 Haygarth, P. M., Warwick, M. S., & House, W. A. (1997). Size distribution of colloidal molybdate
780 reactive phosphorus in river waters and soil solution. *Water Research*, *31*(3), 439–448.
781 https://doi.org/10.1016/S0043-1354(96)00270-9
782 Henderson, R., Kabengi, N., Mantripragada, N., Cabrera, M., Hassan, S., & Thompson, A. (2012).
783 Anoxia-Induced Release of Colloid- and Nanoparticle-Bound Phosphorus in Grassland Soils.
784 *Environmental Science & Technology*, *46*(21), 11727–11734.
785 https://doi.org/10.1021/es302395r
786 Kaplan, D. I., Bertsch, P. M., Adriano, D. C., & Miller, W. P. (1993). Soil-borne mobile colloids as
787 influenced by water flow and organic carbon. *Environmental Science & Technology*, *27*(6),
788 1193–1200. https://doi.org/10.1021/es00043a021
789 Kim, S. T., Cho, H.-R., Jung, E. C., Cha, W., Baik, M.-H., & Lee, S. (2017). Asymmetrical flow field-flow
790 fractionation coupled with a liquid waveguide capillary cell for monitoring natural colloids in
791 groundwater. *Applied Geochemistry*, *87*, 102–107.
792 https://doi.org/10.1016/j.apgeochem.2017.10.010

Klitzke S, Lang F. (2007). Hydrophobicity of soil colloids and heavy metal mobilization: effects of drying. *J Environ Qual*, 36(4), 1187-1193. doi:10.2134/jeq2006.0427

Klitzke, S., Lang, F., & Kaupenjohann, M. (2008*).* Increasing pH releases colloidal lead in a highly contaminated forest soil*. European Journal of Soil Science, 59*, 265-273. doi:10.1111/j.1365-2389.2007.00997.x

Klitzke, S., Lang, G., Kirby, D.J., Lombi, E., & Hamon, R. (2012). Lead, antimony and arsenic in dissolved and colloidal fractions from an amended shooting-range soil as characterised by multi-stage tangential ultrafiltration and centrifugation. *Environmental Chemistry, 9*, 462-473.

Kretzschmar, R., Robarge, W. P., & Amoozegar, A. (1995). Influence of Natural Organic Matter on Colloid Transport Through Saprolite. *Water Resources Research*, *31*(3), 435–445. https://doi.org/10.1029/94WR02676

Kretzschmar, R., Borkovec, M., Grolimund, D., & Elimelech, M. (1999). Mobile Subsurface Colloids and Their Role in Contaminant Transport. In D. L. Sparks (Ed.), *Advances in Agronomy*, *66*, 121–193. https://doi.org/10.1016/S0065-2113(08)60427-7

Lead, J. R., & Wilkinson, K. J. (2006). Aquatic Colloids and Nanoparticles: Current Knowledge and Future Trends. *Environmental Chemistry*, *3*(3), 159. https://doi.org/10.1071/EN06025

Lee, H., Williams, S. K. R., & Giddings, J. C. (1998). Particle size analysis of dilute environmental colloids by flow field-flow fractionation using an opposed flow sample concentration technique. *Analytical Chemistry*, *70*(13), 2495–2503.

Lewandowski, J., & Hupfer, M. (2005). Effect of macrozoobenthos on two-dimensional small-scale heterogeneity of pore water phosphorus concentrations in lake sediments: A laboratory study. *Limnology and Oceanography*, *50*(4), 1106–1118. https://doi.org/10.4319/lo.2005.50.4.1106

Liang, X., Liu, J., Chen, Y., Li, H., Ye, Y., Nie, Z., Su, M., & Xu, Z. (2010). Effect of pH on the release of soil colloidal phosphorus. *Journal of Soils and Sediments*, *10*(8), 1548–1556. https://doi.org/10.1007/s11368-010-0275-6

Liu, J., Yang, J., Liang, X., Zhao, Y., Cade-Menun, B. J., & Hu, Y. (2014). Molecular Speciation of Phosphorus Present in Readily Dispersible Colloids from Agricultural Soils. *Soil Science Society of America Journal*, *78*(1), 47. https://doi.org/10.2136/sssaj2013.05.0159

Luo, X., Yu, L., Wang, C., Yin, X., Mosa, A., Lv, J., & Sun, H. (2017). Sorption of vanadium (V) onto natural soil colloids under various solution pH and ionic strength conditions. *Chemosphere*, *169*, 609–617. https://doi.org/10.1016/j.chemosphere.2016.11.105

Lyvén, B., Hassellöv, M., Turner, D. R., Haraldsson, C., & Andersson, K. (2003). Competition between iron- and carbon-based colloidal carriers for trace metals in a freshwater assessed using flow field-flow fractionation coupled to ICPMS. *Geochimica et Cosmochimica Acta*, *67*(20), 3791–3802. https://doi.org/10.1016/S0016-7037(03)00087-5

Ma, J., Guo, H., & Lei, M. (2017). Disparity of Adsorbed Arsenic Species and Fractions on the Soil and Soil Colloids. *Procedia Earth and Planetary Science*, *17*, 642–645. https://doi.org/10.1016/j.proeps.2016.12.172

Maavara, T., Parsons, C. T., Ridenour, C., Stojanovic, S., Dürr, H. H., Powley, H. R., & Van Cappellen, P. (2015). Global phosphorus retention by river damming. *Proceedings of the National Academy of Sciences of the United States of America*, *112*(51), 15603–15608. https://doi.org/10.1073/pnas.1511797112

837 Maeck, A., DelSontro, T., McGinnis, D. F., Fischer, H., Flury, S., Schmidt, M., Fietzek, P., & Lorke, A.
838 (2013). Sediment Trapping by Dams Creates Methane Emission Hot Spots. *Environmental*
839 *Science & Technology*, *47*(15), 8130–8137. https://doi.org/10.1021/es4003907
840 Majdalani, S., Michel, E., Di-Pietro, L., & Angulo-Jaramillo, R. (2008). Effects of wetting and drying
841 cycles on in situ soil particle mobilization. *European Journal of Soil Science*, *59*(2), 147–155.
842 https://doi.org/10.1111/j.1365-2389.2007.00964.x
843 Maria, E., Crançon, P., Le Coustumer, P., Bridoux, M., & Lespes, G. (2020). Comparison of
844 preconcentration methods of the colloidal phase of a uranium-containing soil suspension.
845 *Talanta*, *208*, 120383. https://doi.org/10.1016/j.talanta.2019.120383
846 Messaud, F. A., Sanderson, R. D., Runyon, J. R., Otte, T., Pasch, H., & Williams, S. K. R. (2009). An
847 overview on field-flow fractionation techniques and their applications in the separation and
848 characterization of polymers. *Progress in Polymer Science*, *34*(4), 351–368.
849 https://doi.org/10.1016/j.progpolymsci.2008.11.001
850 Mills, T. J., Anderson, S. P., Bern, C., Aguirre, A., & Derry, L. A. (2017). Colloid Mobilization and
851 Seasonal Variability in a Semiarid Headwater Stream. *Journal of Environment Quality*, *46*(1),
852 88. https://doi.org/10.2134/jeq2016.07.0268
853 Missong, A., Bol, R., Willbold, S., Siemens, J., & Klumpp, E. (2016). Phosphorus forms in forest soil
854 colloids as revealed by liquid-state 31P-NMR. *Journal of Plant Nutrition and Soil Science*,
855 *179*(2), 159–167. https://doi.org/10.1002/jpln.201500119
856 Missong, A., Holzmann, S., Bol, R., Nischwitz, V., Puhlmann, H., v. Wilpert, K., Siemens, J., & Klumpp,
857 E. (2018). Leaching of natural colloids from forest topsoils and their relevance for
858 phosphorus mobility. *Science of The Total Environment*, *634*, 305–315.
859 https://doi.org/10.1016/j.scitotenv.2018.03.265
860 Mohanty, S. K., Saiers, J. E., & Ryan, J. N. (2015). Colloid Mobilization in a Fractured Soil during Dry–
861 Wet Cycles: Role of Drying Duration and Flow Path Permeability. *Environmental Science &*
862 *Technology*, *49*(15), 9100–9106. https://doi.org/10.1021/acs.est.5b00889
863 Morrison, M. A., & Benoit, G. (2001). Filtration Artifacts Caused by Overloading Membrane Filters.
864 *Environmental Science & Technology*, *35*(18), 3774–3779.
865 https://doi.org/10.1021/es010670k
866 Munkholm, L. J., & Kay, B. D. (2002). Effect of Water Regime on Aggregate-tensile Strength, Rupture
867 Energy, and Friability. *Soil Science Society of America Journal*, *66*(3), 702–709.
868 https://doi.org/10.2136/sssaj2002.7020
869 Murali, R., Murthy, C. N., & Chamyal, L. S. (2012). Characterization of colloids in the late Quaternary
870 sediment sequences of Mahi river basin, Gujarat, India. *Current Science*, 1209–1215.
871 Newman, E. I. (2008). *Applied Ecology and Environmental Management*. John Wiley & Sons.
872 North, R. L., Johansson, J., Vandergucht, D. M., Doig, L. E., Liber, K., Lindenschmidt, K.-E., Baulch, H.,
873 & Hudson, J. J. (2015). Evidence for internal phosphorus loading in a large prairie reservoir
874 (Lake Diefenbaker, Saskatchewan). *Journal of Great Lakes Research*, *41*, 91–99.
875 https://doi.org/10.1016/j.jglr.2015.07.003
876 Orihel, D. M., Baulch, H. M., Casson, N. J., North, R. L., Parsons, C. T., Seckar, D. C. M., &
877 Venkiteswaran, J. J. (2017). Internal phosphorus loading in Canadian freshwaters: A critical
878 review and data analysis. *Journal canadien des sciences halieutiques et aquatiques*, *74*(12):
879 2005-2029. https://doi.org/10.1139/cjfas-2016-0500
880 Pakhomova, S. V., Hall, P. O. J., Kononets, M. Yu., Rozanov, A. G., Tengberg, A., & Vershinin, A. V.
881 (2007). Fluxes of iron and manganese across the sediment–water interface under various

redox conditions. *Marine Chemistry*, *107*(3), 319–331. https://doi.org/10.1016/j.marchem.2007.06.001

Palanques, A., Guillén, J., Puig, P., & Grimalt, J. O. (2020). Effects of flushing flows on the transport of mercury-polluted particulate matter from the Flix Reservoir to the Ebro Estuary. *Journal of Environmental Management*, *260*, 110028. https://doi.org/10.1016/j.jenvman.2019.110028

Pestana, I. A., Azevedo, L. S., Bastos, W. R., & Magalhães de Souza, C. M. (2019). The impact of hydroelectric dams on mercury dynamics in South America: A review. *Chemosphere*, *219*, 546–556. https://doi.org/10.1016/j.chemosphere.2018.12.035

Pettersson, K., Boström, B., & Jacobsen, O. (1988). Phosphorus in sediments—Speciation and analysis. *Hydrobiologia*, *48*(170), 91–101. https://doi.org/10.1007/978-94-009-3109-1_7

Phillips, C. B., Dallmann, J. D., Jerolmack, D. J., & Packman, A. I. (2019). Fine-Particle Deposition, Retention, and Resuspension Within a Sand-Bedded Stream Are Determined by Streambed Morphodynamics. *Water Resources Research*, *55*(12), 10303–10318. https://doi.org/10.1029/2019WR025272

Pokrajac, D., Manes, C., & McEwan, I. (2007). Peculiar mean velocity profiles within a porous bed of an open channel. *Physics of Fluids*, *19*(9), 098109. https://doi.org/10.1063/1.2780193

Ran, Y., Fu, J. M., Sheng, G. Y., Beckett, R., & Hart, B. T. (2000). Fractionation and composition of colloidal and suspended particulate materials in rivers. *Chemosphere*, *41*(1–2), 33–43.

Ranville, J. F., Chittleborough, D. J., Shanks, F., Morrison, R. J., Harris, T., Doss, F., & Beckett, R. (1999). Development of sedimentation field-flow fractionation-inductively coupled plasma mass-spectrometry for the characterization of environmental colloids. *Analytica Chimica Acta*, *381*(2–3), 315–329.

Rapin, A., Rabiet, M., Mourier, B., Grybos, M., & Deluchat, V. (2019a). Sedimentary phosphorus accumulation and distribution in the continuum of three cascade dams (Creuse River, France). *Environmental Science and Pollution Research*. Scopus. https://doi.org/10.1007/s11356-019-07184-6

Rapin, A., Grybos, M., Rabiet, M., Mourier, B., & Deluchat, V. (2019b). Phosphorus mobility in dam reservoir affected by redox oscillations: An experimental study. *Journal of Environmental Sciences*, *77*, 250–263. https://doi.org/10.1016/j.jes.2018.07.016

Regelink, I. C., Voegelin, A., Weng, L., Koopmans, G. F., & Comans, R. N. J. (2014). Characterization of Colloidal Fe from Soils Using Field-Flow Fractionation and Fe K-Edge X-ray Absorption Spectroscopy. *Environmental Science & Technology*, *48*(8), 4307–4316. https://doi.org/10.1021/es405330x

Rothe, M., Frederichs, T., Eder, M., Kleeberg, A., & Hupfer, M. (2014). Evidence for vivianite formation and its contribution to long-term phosphorus retention in a recent lake sediment: A novel analytical approach. *Biogeosciences*, *11*(18), 5169–5180. https://doi.org/10.5194/bg-11-5169-2014

Rothe, M., Kleeberg, A., & Hupfer, M. (2016). The occurrence, identification and environmental relevance of vivianite in waterlogged soils and aquatic sediments. *Earth-Science Reviews*, *158*, 51–64. https://doi.org/10.1016/j.earscirev.2016.04.008

Salim, R., & Cooksey, B. G. (1981). The effect of centrifugation on the suspended particles of river waters. *Water Research*, *15*(7), 835–839. https://doi.org/10.1016/0043-1354(81)90137-8

Schroeder, H., Fabricius, A.-L., Ecker, D., Ternes, T. A., & Duester, L. (2019). Impact of mechanical disturbance and acidification on the metal(loid) and C, P, S mobility at the sediment water interface examined using a fractionation meso profiling ICP-QQQ-MS approach. *Science of*

the Total Environment, *651*, 2130–2138. Scopus. https://doi.org/10.1016/j.scitotenv.2018.09.390

Seaman, J. C., Bertsch, P. M., & Strom, R. N. (1997). Characterization of Colloids Mobilized from Southeastern Coastal Plain Sediments. *Environmental Science & Technology*, *31*(10), 2782–2790. https://doi.org/10.1021/es961075z

Séquaris, J. M., Klumpp, E., & Vereecken, H. (2013). Colloidal properties and potential release of water-dispersible colloids in an agricultural soil depth profile. *Geoderma*, *193–194*, 94–101. https://doi.org/10.1016/j.geoderma.2012.10.014

Shand, C. A., Smith, S., Edwards, A. C., & Fraser, A. R. (2000). Distribution of phosphorus in particulate, colloidal and molecular-sized fractions of soil solution. *Water Research*, *34*(4), 1278–1284.

Shirazi, S., Lin, C. J., & Chen, D. (2010). Inorganic fouling of pressure-driven membrane processes—A critical review. *Desalination*, *250*(1), 236–248. https://doi.org/10.1016/j.desal.2009.02.056

Sinaj, S., Mächler, F., Frossard, E., Faïsse, C., Oberson, A., & Morel, C. (1998). Interference of colloidal particles in the determination of orthophosphate concentrations in soil water extracts. *Communications in Soil Science and Plant Analysis*, *29*(9–10), 1091–1105. https://doi.org/10.1080/00103629809370011

Speth, T. F., Gusses, A. M., & Scott Summers, R. (2000). Evaluation of nanofiltration pretreatments for flux loss control. *Desalination*, *130*(1), 31–44. https://doi.org/10.1016/S0011-9164(00)00072-2

Steiner, Z., Lazar, B., Reimers, C. E., & Erez, J. (2019). Carbonates dissolution and precipitation in hemipelagic sediments overlaid by supersaturated bottom-waters – Gulf of Aqaba, Red Sea. *Geochimica et Cosmochimica Acta*, *246*, 565–580. https://doi.org/10.1016/j.gca.2018.12.007

Stolpe, B., Guo, L., Shiller, A. M., & Aiken, G. R. (2013). Abundance, size distributions and trace-element binding of organic and iron-rich nanocolloids in Alaskan rivers, as revealed by field-flow fractionation and ICP-MS. *Geochimica et Cosmochimica Acta*, *105*, 221–239. https://doi.org/10.1016/j.gca.2012.11.018

Stumm, W., & Morgan, J. J. (1995, October). Aquatic Chemistry: Chemical Equilibria and Rates in Natural Waters, 3rd Edition. *Wiley.*

Sun, S. Q., Cai, H.-Y., Chang, S. X., & Bhatti, J. S. (2015). Sample storage-induced changes in the quantity and quality of soil labile organic carbon. *Scientific Reports*, *5,* 17496. https://doi.org/10.1038/srep17496

Tang, Z., Wu, L., Luo, Y., & Christie, P. (2009). Size fractionation and characterization of nanocolloidal particles in soils. *Environmental Geochemistry and Health*, *31*(1), 1–10. https://doi.org/10.1007/s10653-008-9131-7

Teodoru, C., & Wehrli, B. (2005). Retention of Sediments and Nutrients in the Iron Gate I Reservoir on the Danube River. *Biogeochemistry*, *76*(3), 539–565. https://doi.org/10.1007/s10533-005-0230-6

Tulve, N. S., & Young, T. C. (1999). Isolation and Characterization of the Natural Colloidal Material From the Fox River. *Lake and Reservoir Management*, *15*(3), 231–238. https://doi.org/10.1080/07438149909354120

Turner, B. L., Driessen, J. P., Haygarth, P. M., & Mckelvie, I. D. (2003). Potential contribution of lysed bacterial cells to phosphorus solubilisation in two rewetted Australian pasture soils. *Soil Biology and Biochemistry*, *35*(1), 187–189. https://doi.org/10.1016/S0038-0717(02)00244-4

971 Turner, B. L., Kay, M. A., & Westermann, D. T. (2004). Colloidal phosphorus in surface runoff and
972 water extracts from semiarid soils of the western United States. *Journal of Environmental*
973 *Quality*, *33*(4), 1464–1472.
974 Valipour, R., Boegman, L., Bouffard, D., & Rao, Y. R. (2017). Sediment resuspension mechanisms and
975 their contributions to high-turbidity events in a large lake. *Limnology and Oceanography*,
976 *62*(3), 1045–1065. https://doi.org/10.1002/lno.10485
977 VandeVoort, A. R., Livi, K. J., & Arai, Y. (2013). Reaction conditions control soil colloid facilitated
978 phosphorus release in agricultural Ultisols. *Geoderma*, *206*, 101–111.
979 https://doi.org/10.1016/j.geoderma.2013.04.024
980 Vauthier, C., Cabane, B., & Labarre, D. (2008). How to concentrate nanoparticles and avoid
981 aggregation? *European Journal of Pharmaceutics and Biopharmaceutics*, *69*(2), 466–475.
982 https://doi.org/10.1016/j.ejpb.2008.01.025
983 Vörösmarty, C. J., Meybeck, M., Fekete, B., Sharma, K., Green, P., & Syvitski, J. P. M. (2003).
984 Anthropogenic sediment retention: Major global impact from registered river
985 impoundments. *Global and Planetary Change*, *39*(1), 169–190.
986 https://doi.org/10.1016/S0921-8181(03)00023-7
987 Vuillemin, A., Friese, A., Wirth, R., Schuessler, J. A., Schleicher, A. M., Kemnitz, H., Lücke, A., Bauer, K.
988 W., Nomosatryo, S., von Blanckenburg, F., Simister, R., Ordoñez, L. G., Ariztegui, D., Henny,
989 C., Russell, J. M., Bijaksana, S., Vogel, H., Crowe, S. A., Kallmeyer, J., & Towuti Drilling Project
990 Science Team. (2019). Vivianite formation in ferruginous sediments from Lake Towuti,
991 Indonesia [Preprint]. Biogeosciences, 17, 1955–1973. https://doi.org/10.5194/bg-17-1955-
992 2020
993 Wan, J., and Wilson, J. L. (1994). Colloid transport in unsaturated porous media. *Water Resour*.
994 Res., 30(4), 857– 864. doi:10.1029/93WR03017
995 Wang, K., Zhao, Y., Yang, Z., Lin, Z., Tan, Z., Du, L., & Liu, C. (2018). Concentration and
996 characterization of groundwater colloids from the northwest edge of Sichuan basin, China.
997 *Colloids and Surfaces A: Physicochemical and Engineering Aspects*, *537*, 85–91.
998 https://doi.org/10.1016/j.colsurfa.2017.08.032
999 Wang, W. X., & Guo, L. (2000). Bioavailability of colloid-bound Cd, Cr, and Zn to marine plankton.
1000 *Marine Ecology Progress Series*, *202*, 41–49.
1001 Weißbecker, C., Buscot, F., & Wubet, T. (2017). Preservation of nucleic acids by freeze-drying for
1002 next generation sequencing analyses of soil microbial communities. *Journal of Plant Ecology*,
1003 *10*(1), 81–90. https://doi.org/10.1093/jpe/rtw042
1004 Wildi, W., Dominik, J., Loizeau, J.-L., Thomas, R. L., Favarger, P.-Y., Haller, L., Perroud, A., &
1005 Peytremann, C. (2004). River, reservoir and lake sediment contamination by heavy metals
1006 downstream from urban areas of Switzerland. *Lakes & Reservoirs: Science, Policy and*
1007 *Management for Sustainable Use*, *9*(1), 75–87. https://doi.org/10.1111/j.1440-
1008 1770.2004.00236.x
1009 Wilding, A., Liu, R., & Zhou, J. L. (2004). Validation of cross-flow ultrafiltration for sampling of
1010 colloidal particles from aquatic systems. *Journal of Colloid and Interface Science*, *280*(1),
1011 102–112. https://doi.org/10.1016/j.jcis.2004.07.002
1012 Wilkinson, K. J., & Lead, J. R. (2007). Environmental Colloids and Particles: Behaviour, Separation and
1013 Characterisation. *Wiley.*
1014 Wolthoorn, A., Temminghoff, E. J. M., Weng, L., & van Riemsdijk, W. H. (2004). Colloid formation in
1015 groundwater: Effect of phosphate, manganese, silicate and dissolved organic matter on the

dynamic heterogeneous oxidation of ferrous iron. *Applied Geochemistry*, *19*(4), 611–622. https://doi.org/10.1016/j.apgeochem.2003.08.003

Woszczyk, M. (2016). Precipitation of calcium carbonate in a shallow polymictic coastal lake: Assessing the role of primary production, organic matter degradation and sediment mixing. *Oceanological and Hydrobiological Studies*, *45*(1), 86–99. https://doi.org/10.1515/ohs-2016-0009

Wu, Y., Ma, H. L., & Peng, Y. Z. (2018). [Effects of storage temperature and time on the contents of different nitrogen forms in fresh soil samples.]. *Ying Yong Sheng Tai Xue Bao = The Journal of Applied Ecology*, *29*(6), 1999–2006. https://doi.org/10.13287/j.1001-9332.201806.035

Xu, H., Ji, L., Kong, M., Xu, M., & Lv, X. (2019). Abundance, chemical composition and lead adsorption properties of sedimentary colloids in a eutrophic shallow lake. *Chemosphere*, *218*, 534–539. https://doi.org/10.1016/j.chemosphere.2018.11.147

Yan, C., Nie, M., Lead, J. R., Yang, Y., Zhou, J., Merrifield, R., & Baalousha, M. (2016). Application of a multi-method approach in characterization of natural aquatic colloids from different sources along Huangpu River in Shanghai, China. *Science of The Total Environment*, *554–555*, 228–236. https://doi.org/10.1016/j.scitotenv.2016.02.198

Yan, J., Meng, X., & Jin, Y. (2017). Size-Dependent Turbidimetric Quantification of Suspended Soil Colloids. *Vadose Zone Journal*, *16*(5), 0. https://doi.org/10.2136/vzj2016.10.0098

Zang, L., Tian, G.-M., Liang, X.-Q., He, M.-M., Bao, Q.-B., & Yao, J.-H. (2013). Profile Distributions of Dissolved and Colloidal Phosphorus as Affected by Degree of Phosphorus Saturation in Paddy Soil. *Pedosphere*, *23*(1), 128–136. https://doi.org/10.1016/S1002-0160(12)60088-5

Zhang, B., Fang, F., Guo, J., Chen, Y., Li, Z., & Guo, S. (2012). Phosphorus fractions and phosphate sorption-release characteristics relevant to the soil composition of water-level-fluctuating zone of Three Gorges Reservoir. *Ecological Engineering*, *40*, 153–159. https://doi.org/10.1016/j.ecoleng.2011.12.024

Zhang, S., Yi, Q., Buyang, S., Cui, H., & Zhang, S. (2019). Enrichment of bioavailable phosphorus in fine particles when sediment resuspension hinders the ecological restoration of shallow eutrophic lakes. *Science of The Total Environment*, *710*, 135672. https://doi.org/10.1016/j.scitotenv.2019.135672

Zirkler, D., Lang, F., & Kaupenjohann, M. (2012). "Lost in filtration"—The separation of soil colloids from larger particles. *Colloids and Surfaces A: Physicochemical and Engineering Aspects*, *399*, 35–40. https://doi.org/10.1016/j.colsurfa.2012.02.021

Table captions

Table 1: Application of filtration, centrifugation and their combination for colloid separation.

Note: CNA: composite cellulose nitrate/acetate membrane, DI: deionized water, nd: not determined, OM: organic matter, S/L: solid-liquid ratio by dry weight per volume, UC: ultra-centrifugation, UF: ultrafiltration, UPW: ultrapure water

Table 2: Characteristics of sediment collected in the Champsanglard dam reservoir.

Figure captions

Figure 1: Colloid extraction and separation protocols applied on wet sediment.

Figure 2: Variation in dry mass of the colloidal fraction sized 0.2 - 1 µm by means of different colloid separation protocols. The error bar depicted 1 SD.

Figure 3: Effect of colloid separation protocols on the size distribution of the water-mobilizable fraction smaller than 1 µm, except for protocol "e", which presents the 0.2 - 1 µm fraction size. The error bar depicted 1 SD.

Figure 4: Distribution of water-mobilizable phosphorus extracted from wet sediment using five separation protocols. Large colloidal P sized from 0.2 – 1 µm. Small colloidal P sized smaller than 0.2 µm. Dissolved P represented dissolved inorganic phosphate in fraction smaller than 0.2 µm. The error bar depicted 1 SD.

Figure 5: Impacts of colloid separation methods on the elemental composition, expressed per dry mass of sediment for: a) large colloidal fraction (0.2 - 1 µm), and b) fraction below 0.2 µm; versus c) the concentration per dry mass of large colloids (0.2 - 1 µm). The error bar depicted 1 SD.

Figure 6: Effect of the rewetting of previously air-, oven-, and freeze-dried sediments on the dry mass of colloids sized 0.2 - 1 µm. The employed colloid separation protocol was high-speed centrifugation combined with filtration (i.e. protocol “d”, Fig. 1). The error bar depicted 1 SD.

Figure 7: Effect of the rewetting of previously air-, oven-, and freeze-dried sediments on the size distribution of the water-mobilizable fraction smaller than 1 µm. The employed colloid separation protocol was high-speed centrifugation combined with filtration (i.e. protocol “d”, Fig. 1). The error bar depicted 1 SD.

Figure 8: Impacts of the rewetting of previously air-, oven-, and freeze-dried sediments on the elemental composition, expressed per dry mass of sediment of: a) large colloidal fraction (0.2 - 1 µm), and b) fraction below 0.2 µm; versus c) the concentration per dry mass of large colloids (0.2 - 1 µm). Extraction using the high-speed centrifugation protocol combined with filtration (i.e. protocol “d”, Fig. 1). The error bar depicted 1 SD.

Figure 9: Distribution of water-mobilizable phosphorus extracted from wet and rewetted previously air-, oven-, and freeze-dried sediments using the high-speed centrifugation protocol combined with filtration (i.e. protocol “d”, Fig. 1). Large colloidal P sized from 0.2 – 1 µm. Small colloidal P sized smaller than 0.2 µm. Dissolved P represented dissolved inorganic phosphate in fraction smaller than 0.2 µm. The error bar depicted 1 SD.

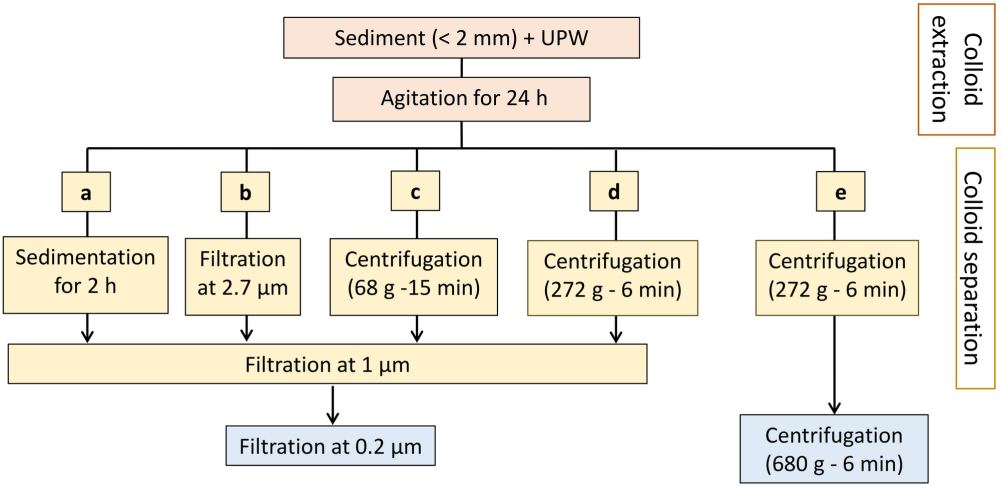

Protocol	Pre-separation	Separation of fraction < 1 µm	Separation of fraction < 0.2 µm
a	Sedimentation	Filtration 1 µm	Filtration 0.2 µm
b	Filtration 2.7 µm	Filtration 1 µm	Filtration 0.2 µm
c	Centrifugation 68 g	Filtration 1 µm	Filtration 0.2 µm
d	Centrifugation 272 g	Filtration 1 µm	Filtration 0.2 µm
e	None	Centrifugation 272 g	Centrifugation 680 g

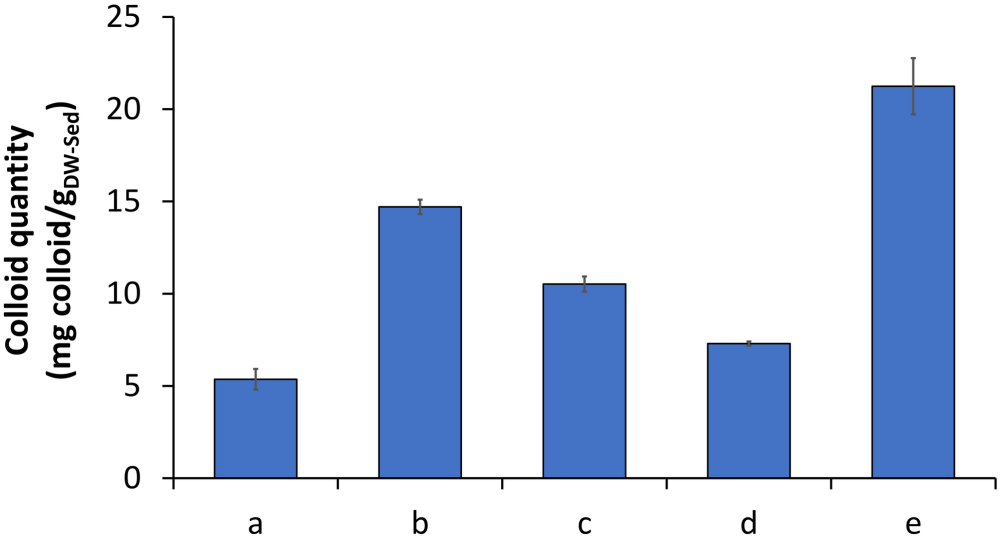
Colloid quantity
(mg colloid/g$_{DW-Sed}$)
25
20
15
10
5
0
a
b
c
d
e

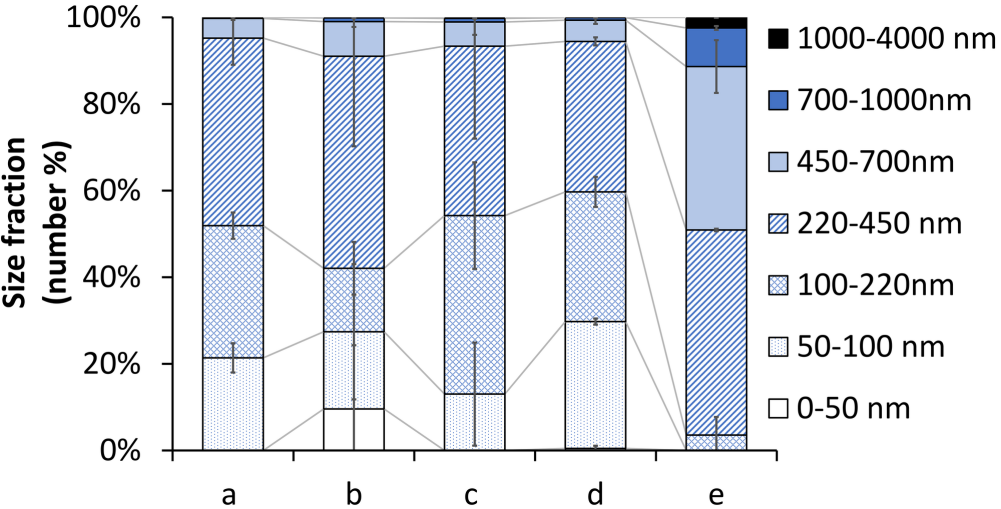
Size fraction (number %)
100%
80%
60%
40%
20%
0%
a
b
c
d
e
1000-4000 nm
700-1000nm
450-700nm
220-450 nm
100-220nm
50-100 nm
0-50 nm

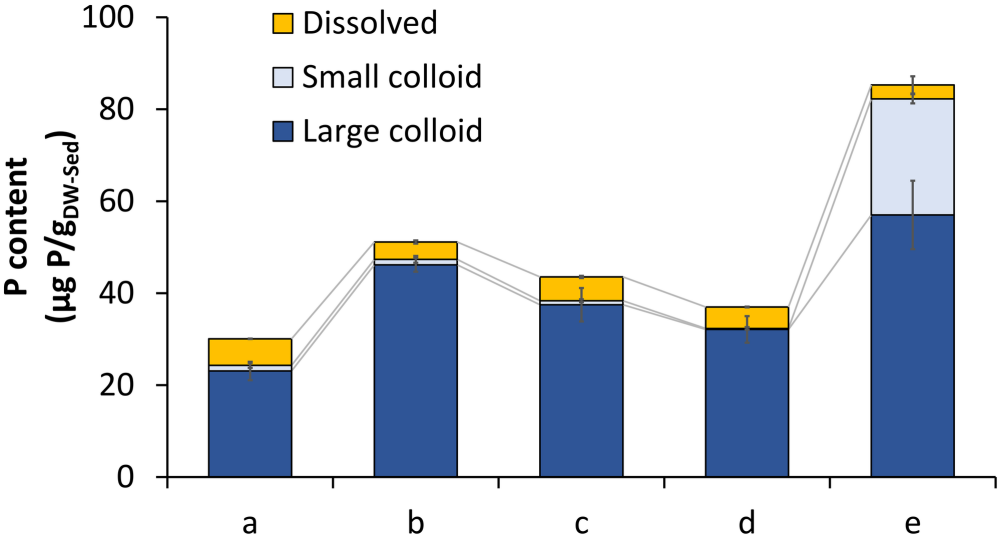
Dissolved
Small colloid
Large colloid
P content
(µg P/g$_{DW-Sed}$)
100
80
60
40
20
0
a
b
c
d
e

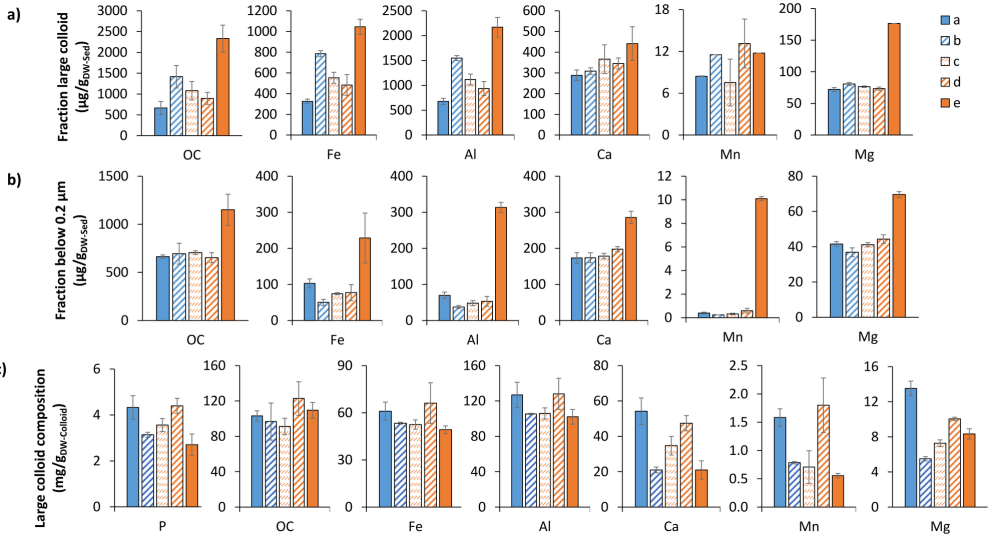
a)
Fraction large colloid (µg/g_DW-Soil)
OC
Fe
Al
Ca
Mn
Mg
a
b
c
d
e
b)
Fraction below 0.2 µm (µg/g_DW-Soil)
OC
Fe
Al
Ca
Mn
Mg
c)
Large colloid composition (mg/g_DW-Colloid)
P
OC
Fe
Al
Ca
Mn
Mg

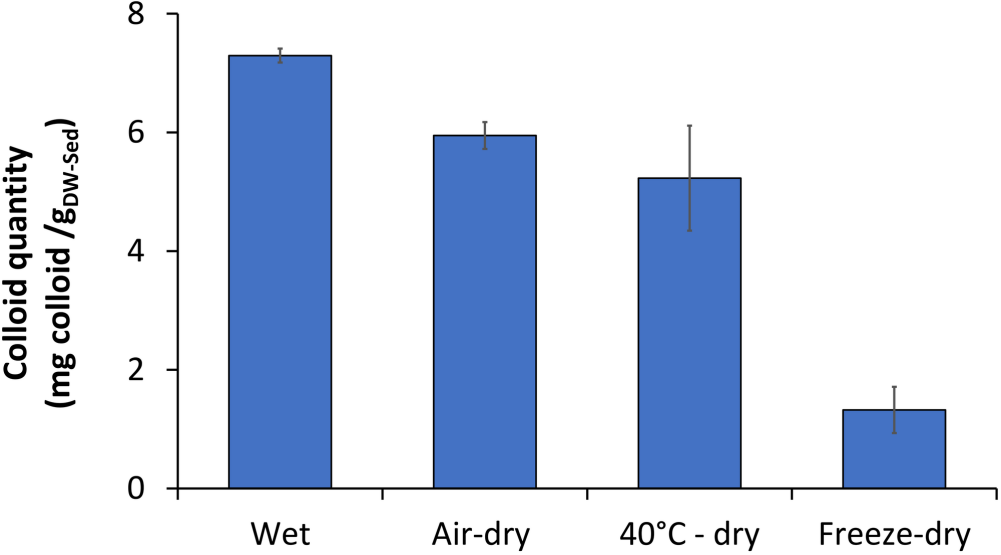
Colloid quantity
(mg colloid /g$_{DW-Sed}$)
8
6
4
2
0
Wet
Air-dry
40°C - dry
Freeze-dry

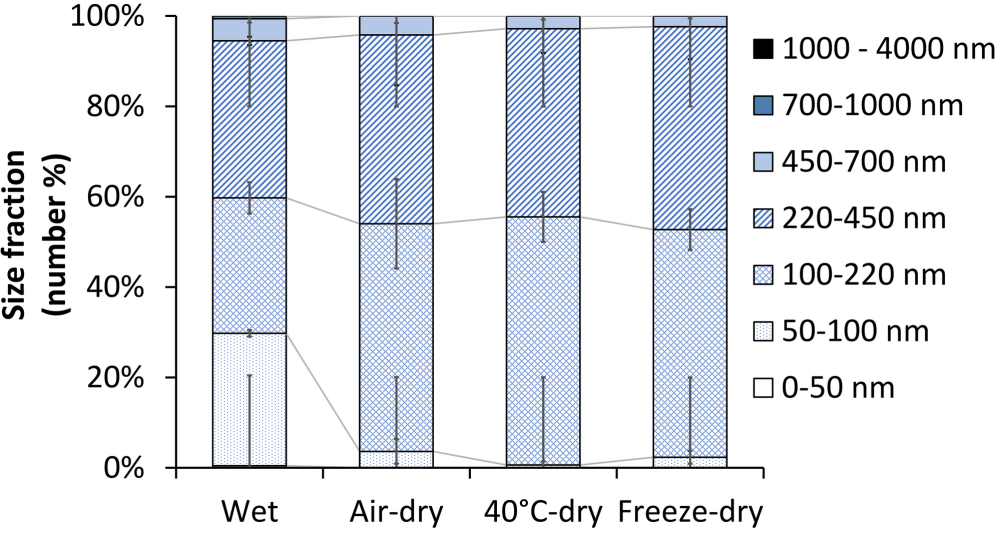
Size fraction (number %)
100%
80%
60%
40%
20%
0%
Wet
Air-dry
40°C-dry
Freeze-dry
1000 - 4000 nm
700-1000 nm
450-700 nm
220-450 nm
100-220 nm
50-100 nm
0-50 nm

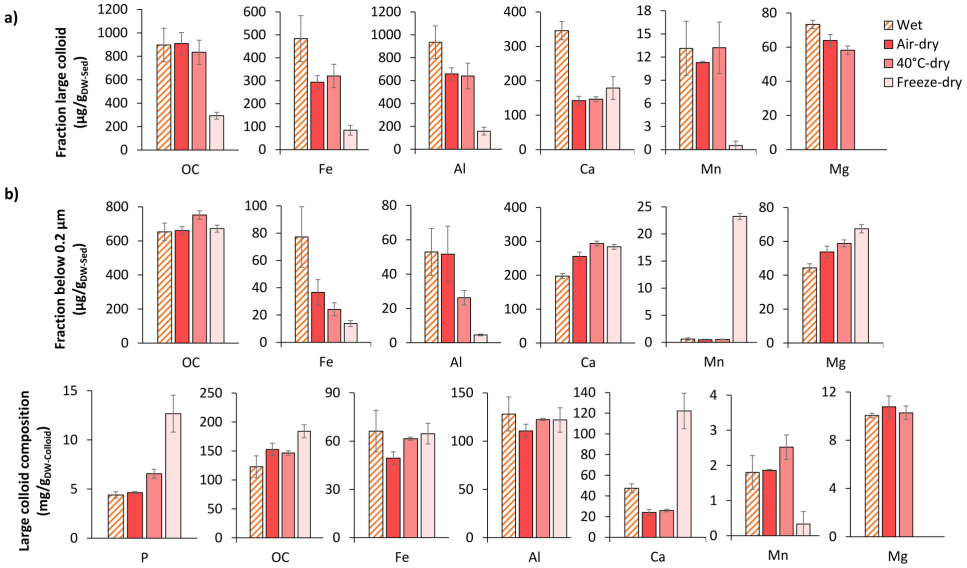
a)
Fraction large colloid (µg/gDW-Soil)
Wet
Air-dry
40°C-dry
Freeze-dry
OC
Fe
Al
Ca
Mn
Mg
b)
Fraction below 0.2 µm (µg/gDW-Soil)
OC
Fe
Al
Ca
Mn
Mg
c)
Large colloid composition (mg/gDW-Colloid)
P
OC
Fe
Al
Ca
Mn
Mg

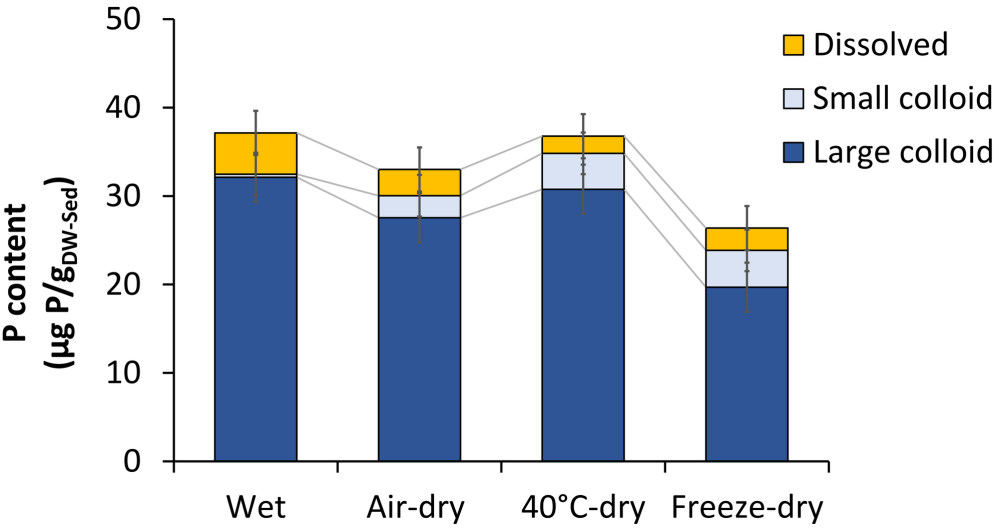
50
40
30
20
10
0
P content
(µg P/g$_{DW-Sed}$)
Dissolved
Small colloid
Large colloid
Wet
Air-dry
40°C-dry
Freeze-dry

Authors	Matrix	Storage	Extraction method	Separation method		Colloid size	Colloid quantitative method	Colloid quantity
				Principal	Operation			
Kretzschmar et al. (1995)	Georgeville clay loam soil Fraction: nd	24 h - soaked soil	S/L: nd Dispersant: DI Mode: agitation (2 h)	Wet sieving Centrifugation	nd	0.05 - 0.5 µm	nd	nd
Haygarth et al. (1997)	River and soil waters Fraction: nd	Store at 4°C	nd	Filtration	Membrane filtration: 0.45, 0.22, 0.1 and 0.025 µm (CNA) UF: 10 kDa and 1 kDa at 276 kPa	nd	nd	nd
Bergendahl & Grasso (1998)	Soil Fraction: < 6 mm	Store at 4°C	S/L: 1/20 Dispersant: acetate buffer (pH 5); UPW Mode: agitation at 30 rpm (6, 18, 24 and 36 h)	Filtration	Membrane filtration: 0.7 µm (glass fiber filter)	0.47 - 0.95 µm (peak at 0.65 µm)	nd	nd
Sinaj et al. (1998)	Soil Fraction: nd	nd	S/L: 1/10 Dispersant: nano pure water Mode: agitation (17 h)	Centrifugation combined filtration	Centrifugation: 2500 g (15 min) Filtration: 0.45, 0.2 or 0.025 µm	0.025 - 0.45 µm	Air dry	260 - 1320 mg/kg soil
Shand et al. (2000)	Soil rich in OM Fraction: < 6 mm	Air-dry	nd	Centrifugation and successive filtrations	Centrifugation: 1000 g (60 min) Filtration: 1.6 µm, 1.2 µm, 0.7 µm, 0.45 µm and 0.22 µm UF: 100, 10 and 1 kDa	0.22 - 1.2 µm	nd	nd
Turner et al. (2004)	Soil Fraction: < 2 mm	Air-dry (7 days)	S/L: 1/100 Dispersant: DI	Centrifugation, filtration, UF	Centrifugation: 3000g (15 min) Filtration: 1, 0.4, 0.2 and 0.1 µm UF: 100, 10, 3 and 1 kDa	1 kDa - 1 µm	nd	nd

			Mode: sonication at 650 W (5 min)					
Klitzke et al. (2008)	Soil Fraction: < 2 mm	nd	S/L: 1/10 Dispersant: water Mode: agitation (12 h)	Filtration and UC	Filtration: 1.2 µm UC: particle diameter 4 and 10 nm	250 - 900 nm	nd	nd
Liang et al. (2010)	Soil Fraction: < 2 mm	Air-dry	S/L: 1/8 Dispersant: DI Mode: agitation at 160 rpm (24 h)	Centrifugation, filtration and UC	Centrifugation: 3000 g (10 min) Filtration: 1 µm UC: 300,000 g (2h)	nd	nd	nd
Murali et al. (2012)	River sediment Fraction: nd	Air-dry	S/L: 1/5 Dispersant: distilled water Mode: agitation (24 h)	Centrifugation	750 rpm (15 min)	20 - 300 nm	Dry at 100 °C	200 - 2400 mg/L
Zirkler et al. (2012)	Soil Fraction: < 2 mm	nd	S/L: 1/10 Dispersant: DI Mode: agitation at 15 rpm (16 h)	Filtration, centrifugation, UC	Filtration: 1.2 and 1 µm Centrifugation: 78 g UC: 124,000 g (1 h 17 min)	< 1 µm	Turbidity	Maximum: 1200 NFU
Séquaris et al. (2013)	Ruptic and siltic soil Fraction: < 2 mm	Air-dry	S/L: 1/10 Dispersant: DI Mode: agitation at 150 rpm (6 h)	Sedimentation and centrifugation	Sedimentation: 12 h Centrifugation: 10,000 g (90 min)	499 - 790 nm	nd	nd

VandeVoort et al. (2013)	Sandy loam soil Fraction: < 2 µm	Air-dry	S/L: 1/20 Dispersant: nd Mode: agitation (48 h)	Centrifugation and filtration	Centrifugation: 2300 g (3 min) Filtration: 0.2 µm	0.2 - 0.41 µm	nd	nd
Zang et al. (2013)	Gleyed paddy soil Fraction: < 2 mm	Air-dry	S/L: 1/20 Dispersant: DI Mode: agitation (16 h)	Centrifugation, filtration and UC	Centrifugation: 3000 g (10 min) Filtration: 1 µm UC: 300,000 g (1h)	nd	nd	nd
Buettner et al. (2014)	Mineral soil Fraction: nd	Store at 4°C	S/L: 1/10 Dispersant: 2 mM KCl Mode: agitation at 120 rpm (2 h)	Successive centrifugation and UF	Centrifugation: 3195 g (3 min); 21,169 g (24 min) UF: 10 kDa (14,000 rpm, 10 min)	2.3 - 430 nm	nd	nd
Liu et al. (2014)	Ultisol soil Fraction: nd		S/L: 1/8 Dispersant: DI Mode: agitation (24 h)	Centrifugation, filtration and UC	Centrifugation: 3000 g (10 min) Filtration: 1 µm UC: 300,000 g (2 h)	0.02 – 1 µm	Dry at 100°C	nd
Missong et al. (2016)	Cambisol soil Fraction: < 2 mm	Fresh sample	S/L: 1/8 Dispersant: UPW Mode: agitation at 150 rpm (6 h)	Sedimentation, centrifugation and UC	Sedimentation: 15 - 20 min Centrifugation: 4000 g (4 min) UC: 14,000 g (60 min)	350 - 400 nm (average size)	Freeze drying	nd
Luo et al. (2017)	Soil Fraction: < 2 mm	Air-dry	S/L: nd Dispersant: nd Mode: agitation (2 h); sonication (30 min)	Sedimentation	Settle 24 h	96 - 181 nm (mean diameter)	nd	nd

Ma et al. (2017)	Forest land soil Fraction: 11.5 µm	nd	S/L: nd Dispersant: UWP Mode: sonication	Sedimentation and filtration	Sedimentation: nd Filtration: 1.2 µm	257.4 nm (Average size)	nd	nd
Mills et al. (2017)	Ground water and soil Fraction: nd	nd	S/L: nd Dispersant: DI Mode: agitation (1 h)	Filtration and centrifugation	Filtration: 0.45 µm Centrifugation: 8000 rpm (4.5 h)	0.02 - 0.45 µm	nd	nd
Yan et al. (2017)	Soil Fraction: < 0.05 mm	Air-dry	S/L: 1/10 Dispersant: DI Mode: agitation (24 h); sonication (15 min)	Successive centrifugation	Centrifugation: 221 g (8 min); 884 g (10 min); 22,095 g (8 min)	< 0.1 µm 0.1 - 0.45 0.45 - 1 µm	Dry at 105°C	nd 46.9 mg/L 29.2 mg/L
Gu et al. (2018)	Luvisol soil (leachate) Fraction: < 2 mm	Air-dry	S/L: nd Dispersant: 10 mM NaCl Mode: agitation (24 h); sonication (15 min)	Filtration and UF	Filtration: 0.45 µm UF: 30 kDa and 5 kDa (3400 g, 15 and 25 min, respectively)	5 kDa - 30 kDa 30 kDa - 0.45 µm	nd	nd
Xu et al. (2019)	Lake sediment Fraction: < 2 mm	Freeze-dry	S/L: 3/20 Dispersant: $NaHCO_3$ Mode: sonication	Sedimentation, UF and UC	Sedimentation: nd UF: 1 kDa (concentration factor: 25) UC: 15,000 g (10 min)	30 - 200 nm	nd	nd

	pH	D_{50}	Particle density	~~Siccity~~ Water loss on drying	OM*	P	Fe	Al	Ca	Mn	Mg
		µm	g/cm^3	%	%	$mg/g_{DW\text{-}Sed}$	$mg/g_{DW\text{-}Sed}$	$mg/g_{DW\text{-}Sed}$	$mg/g_{DW\text{-}Sed}$	$mg/g_{DW\text{-}Sed}$	$mg/g_{DW\text{-}Sed}$
Sediment	6.4 ± 0.2	19 ± 1	2.417	~~18.4~~81.6	19 ± 1	1.43 ± 0.01	79 ± 1	136 ± 4	8.5 ± 0.5	1.5 ± 0.1	17.2 ± 0.0

*OM - organic matter